

3-2016

# Development of a Direct Activity Probe for Rho-Associated Protein Kinase

Maia Kelly

University of Nebraska-Lincoln, maia.kelly@huskers.unl.edu

Follow this and additional works at: <http://digitalcommons.unl.edu/chemistrydiss>



Part of the [Chemistry Commons](#)

---

Kelly, Maia, "Development of a Direct Activity Probe for Rho-Associated Protein Kinase" (2016). *Student Research Projects, Dissertations, and Theses - Chemistry Department*. 67.  
<http://digitalcommons.unl.edu/chemistrydiss/67>

This Article is brought to you for free and open access by the Chemistry, Department of at DigitalCommons@University of Nebraska - Lincoln. It has been accepted for inclusion in Student Research Projects, Dissertations, and Theses - Chemistry Department by an authorized administrator of DigitalCommons@University of Nebraska - Lincoln.

Development of a Direct Activity Probe for Rho-Associated  
Protein Kinase

by

Maia Kelly

A THESIS

Presented to the Faculty of  
The Graduate College at the University of Nebraska  
In Partial Fulfillment of Requirements  
For the Degree of Master of Science

Major: Chemistry

Under the Supervision of Professor Cliff Stains

Lincoln, Nebraska

March, 2016

# Development of Direct Activity Probe for Rho-Associated Protein Kinase

Maia Kelly, M.S.

University of Nebraska, 2016

Advisor: Cliff I. Stains

Hepatocellular carcinoma (HCC) is an extremely aggressive form of liver cancer with a low survival rate due to high recurrence. Increases in Rho-associated Protein Kinase (ROCK) activity are correlated with a more aggressive, metastatic phenotype associated with advanced HCC. Inhibitors for ROCK have shown potential for the reduction of this metastatic phenotype of HCC. We outline the design and optimization of a direct activity sensor for ROCK that utilizes a phosphorylation-sensitive sulfonamido-oxine fluorophore, termed Sox, and is capable of reporting on the inhibition of ROCK. This CSox-based activity probe utilizes chelation-enhanced fluorescence (ex. = 360 nm and em. = 485 nm) between the proximal phosphorylated residue,  $Mg^{2+}$  and the Sox fluorophore. This allows for the direct and continuous monitoring of phosphorylation of the peptide-based probe over time. The sensitivity of the optimal CSox-based probe, ROCK-S1, was detected to be 10 pM of recombinant enzyme. Using this probe we demonstrate the ability to directly and rapidly assess a pilot small molecule library for inhibitors of ROCK2, using a robotics platform. In a step towards applying our probe in complex biological systems, we identify the optimal conditions for monitoring ROCK2 while inhibiting off-target enzymes (PKC $\alpha$ , PKA, and PAK). Our work provides a sensitive assay platform for ROCK activity that is compatible to HTS and could potentially be used to interrogate ROCK activity in heterogeneous biological samples.

# Contents

List of Abbreviations .....	3
Chapter 1- Introduction.....	4
1.1 Structural and mechanistic characteristics of protein kinases.....	4
1.2 Current methodology for the detection of protein kinase activity .....	6
1.3 The protein kinase ROCK drives aggressive phenotypes in HCC.....	10
1.2 Biology of ROCK.....	12
1.5 The need for a ROCK probe .....	17
Chapter 2 – Design and Optimization of CSox-Based Sensor for Rho-Associated Protein Kinase and Implementation in High Throughput Screening .....	19
2.1 Introduction .....	19
2.2 Results and discussion.....	20
2.2.1 Rational design and characterization of preliminary ROCK activity probes ...	20
2.2.2 Evaluation of probe efficiency for ROCK2.....	25
2.2.3 ROCK-S1 limit of detection for ROCK2 .....	28
2.2.4 ROCK-S1 can report on ROCK2 inhibition.....	30
2.2.5 Optimization of HTS conditions.....	32
2.2.6 Selectivity of ROCK-S1 .....	39
2.3 Experimental .....	42
2.3.1 General reagents, instrumentation, and procedures.....	42
2.3.2 Peptide synthesis.....	42
2.3.3 Determination of Mg <sup>2+</sup> affinity and fold fluorescence increase .....	44
2.3.4 Recombinant enzyme assays .....	44
2.3.5 High-throughput screening.....	45
2.4 Conclusions and Future Directions .....	47
Appendix A.....	48
References.....	62

## List of Abbreviations

CHEF	Chelation-Enhanced Fluorescence
CSox	Cysteine-Sox
DTT	Dithiothreitol
EGTA	Ethylene Glycol Tetraacetic Acid
HCC	Hepatocellular Carcinoma
HTS	High Throughput Screening
K <sub>D</sub>	Equilibrium Disassociation Constant
MLC	Myosin Light Chain
PBS	Phosphate-buffered saline
ROCK	Rho-associated Protein Kinase
Sox	Sulfonamido-oxine
IC <sub>50</sub>	Half Maximal Inhibitory Concentration

## Chapter 1- Introduction

### 1.1 Structural and mechanistic characteristics of protein kinases

Protein kinases are essential for the regulation of signaling pathways through phosphorylation, a post-translational modification. Phosphorylation of protein kinases is crucial for various cellular processes, including cell growth, cell motility, and apoptosis.<sup>1</sup> Protein kinases accomplish this post-translational modification through the transfer of  $\gamma$ -phosphate from ATP to a serine, threonine, or tyrosine residue (Figure 1-1).<sup>2</sup> However the phosphorylation state of a protein kinase does not always correlate to activity levels.<sup>3</sup> Other post-translational modifications have been shown to modify kinase activity. Dysregulations of kinase activity can lead to, or be the result of, certain disease states.<sup>4</sup> Protein kinase sensors that can directly and continually assess protein kinase activity are needed for both monitoring aberrant activity and identifying true inhibitors of protein kinases.<sup>5</sup> The ability to monitor kinase activity in real time will lead to an enhanced understanding of the mechanisms of disease, as well as an increased ability to inhibit specific aspects of disease states.

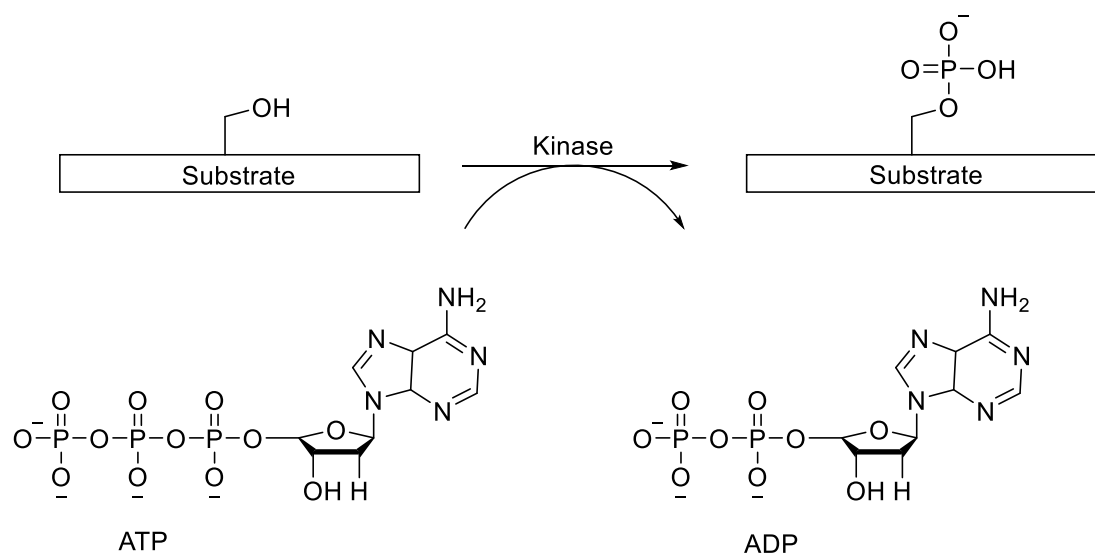


**Figure 1-1.** Protein kinases catalyze the transfer of the  $\gamma$ -phosphate on ATP to the target substrate.

## 1.2 Current methodology for the detection of protein kinase activity

Currently, there are multiple techniques for indirectly or discontinuously probing protein kinase activity. Many of these techniques utilize radioactivity, costly reagents, or specialized equipment that can make implementation, on a large scale, cost prohibitive. An ideal technique for assessing protein kinase activity would have the capability to monitor the activity directly and continuously in a High Throughput Screening (HTS) format. In addition, analytical probes capable of detecting kinase activity in homogeneous biological samples would be desirable.

One common assay for the assessment of protein kinase activity is a radiometric-based assay that monitors the transfer of a radiolabelled  $\gamma$ -phosphate from ATP to the substrate, making it broadly applicable to assessing kinase activity.<sup>6</sup> The activity of the protein kinase is then assessed through scintillation counting of the radiolabeled peptide substrate. In this method the protein kinase activity is monitored indirectly, discontinuously, and cannot be practically implemented in HTS. Radiolabelling ATP is also not a compatible method for measuring kinase activity in cell lysates due to the large number of cellular components and other kinases that utilize ATP.

A more specific approach to assessing protein kinase activity can be found with immuno-based assays. The use of antibodies considerably increases the specificity of the sensor, although also increases the cost. Western Blotting is one example of a common antibody-based assessment of protein kinase activity. This method requires phospho-specific antibodies in order to probe the phosphorylation state of the protein kinase. In some cases, these antibodies are not available or require the probing of a downstream target of the kinase, such as in the case of ROCK. Western blotting is also indirect,

discontinuous, and impractical for HTS. However this method can be used with cell lysates and tissue homogenates.

Another approach to monitoring kinase activity that is utilized in HTS is immuno-fluorescent assays such as ALPHA Screen (Amplified Luminescence Proximity Homogeneous Assay).<sup>7</sup> This immuno-fluorescent approach combines the strength of luminescent small molecules with the specificity of antibodies to create sensors that are able to be implemented in HTS and complex systems, such as cell lysates. ALPHA Screen utilizes a specific GST-tagged peptide substrate for the target on a GSH coated donor bead and acceptor bead coated with antibodies that recognize phosphorylation of the peptide substrate. When the donor bead is excited at 680nm by a laser, a photosensitizer, phthalocyanine, that is present in the donor beads produce singlet oxygen molecules that react with thioxene derivatives and dyes contained in the acceptor beads. This results in emission that can be measured between 520 and 620 nm. ALPHA Screen is a direct activity assay that can be implemented in HTS but is discontinuous and requires time points to be collected in order to obtain rates.

The Imperiali lab has previously reported multiple protein kinase sensors that utilize chelation-enhanced fluorescence (CHEF) for direct and continuous reporting of kinase activity. These sensors utilize a sulfonamido-oxine (Sox) fluorophore that is bound to a specific peptide substrate through a modified amino acid, cysteine. This modified amino acid is placed in the +2 or -2 position of the site of phosphorylation for the  $Mg^{2+}$  binding site to be in an optimal configuration (Figure 1-2). The phosphorylation of the Sox sensor leads to an increase in affinity for  $Mg^{2+}$ . This sensing modality utilizes CHEF between the phosphorylated residue on the specific peptide substrate,  $Mg^{2+}$ , and

the Sox fluorophore. The non-phosphorylated peptide sensor has relatively weak  $Mg^{2+}$  binding ( $100 \text{ mM} < K_D < 300 \text{ mM}$ ), compared to the affinity of  $Mg^{2+}$  for the phosphorylated peptide sensor ( $4 \text{ mM} < K_D < 20 \text{ mM}$ ). The increase of fluorescence over time correlates to the rate of phosphorylation of the probe by the protein kinase.<sup>8</sup>

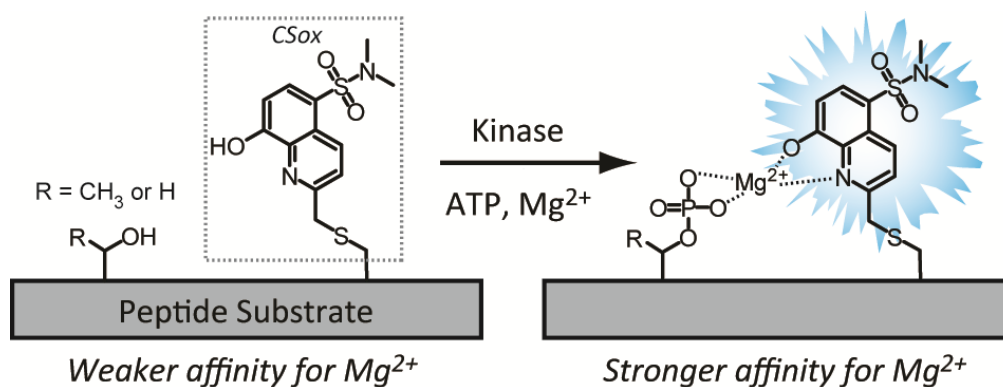


**Figure 1-2.** A modified amino acid, CSox, is integrated into a known peptide substrate for a target kinase. After phosphorylation of the peptide substrate, CHEF between Mg<sup>2+</sup>, Sox, and the phosphorylated residue can be monitored using 360 nm excitation and 485 nm emission.

Unlike some of the previously described assay formats, Sox sensors are able to produce robust fluorescence increases in the presence of physiologically relevant concentrations of  $Mg^{2+}$  (0.5-5 mM)<sup>9</sup> and ATP (0.8-1 mM).<sup>10,11</sup> Upon phosphorylation, the sensors can exhibit a 2—10 fold increase in fluorescence. The Sox sensors are also capable of HTS and measuring the activity of a kinase of interest in cell lysates.<sup>12,13,14,15</sup> This format also causes minimal interference of substrate binding and kinase activity. The Dalby laboratory has utilized the Sox sensors for HTS to discover novel inhibitors of eEF-2K using a 32,960 compound library. The  $IC_{50}$  was determined for the top 2 compounds using a Sox sensor and found to be in the micro-molar range, which was confirmed by radiometric and luminescence assays.<sup>16</sup>

### **1.3 The protein kinase ROCK drives aggressive phenotypes in HCC**

Hepatocellular Carcinoma (HCC) is a highly aggressive and the most common form of liver cancer which can be caused from anabolic steroids, aflatoxins, alcohol, cirrhosis, hemochromatosis, Hepatitis A, and Hepatitis B.<sup>17</sup> In addition, HCC is the third leading cause of death from cancer and has a bleak, five-year survival rate of 15%. The low survival rate has multiple contributing factors but is primarily due to the recurrence of the cancer after treatment (Figure 1-3).<sup>18</sup> Intrahepatic metastasis is one type of recurrence of HCC and is associated with progression to more aggressive phenotypes. Despite our knowledge of genetic mutations associated with HCC, there is relatively little known about the molecular mechanisms that drive this disease at the biochemical level.<sup>19</sup> Nonetheless, one possible route to treatment of advanced disease would be inhibition of the molecules responsible for metastatic HCC. Such treatment could, potentially, increase survival rate.

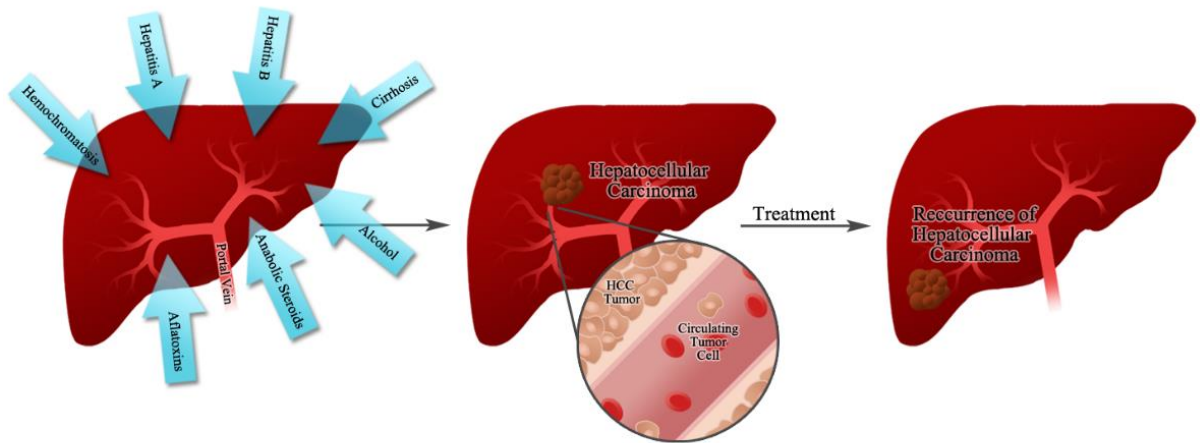


**Figure 1-3.** Hepatocellular carcinoma can be brought on by many factors and has a very low survival rate due to the high probability of recurrence. Intrahepatic metastasis is thought to proceed via the portal vein, as shown.

Cancer metastasis involves multiple steps each of which are potential targets for therapeutic intervention.<sup>20</sup> These steps include primary malignance, cellular detachment, dissemination, and finally proliferation as new tumors. In the case of intrahepatic metastasis, it is suggested that the process of dissemination occurs via the portal vein, and the proliferation of new tumors is localized to the initial environment of the cancer (Figure 1-3).<sup>21</sup> Due to the localization of the metastasis, the initial step of cellular detachment and cell motility has been identified as a target for potential inhibition. Therefore, significant efforts have been undertaken to identify signaling molecules that regulate the metastatic potential of HCC.

Evidence as to the role of ROCK in HCC has been growing. Two HCC cell lines were found to produce intrahepatic metastasis in mice, Li7 and KYN-2.<sup>19</sup> These cell lines also exhibited increased cell motility. The increased cell motility in both cell lines was found to be reduced with C3 exoenzyme, a known specific Rho inhibitor. Li7 was also stably transfected to have a defective mutant without ROCK. This newly transfected knockdown cell line had a drastically decreased percentage of motile cells. These data suggest that ROCK might mediate cell motility, at least in this cell line. In KYN-2 a cell transfectant without ROCK was not able to be established. This adds to the evidence that ROCK might be responsible for cell proliferation, especially in this cell line.

## **1.2 Biology of ROCK**

ROCK has been identified as a critical regulator of cell motility and metastatic potential in HCC.<sup>22</sup> ROCK is a serine/threonine protein kinase that is a member of the AGC family. ROCK1 and ROCK2 are two isoforms that comprise the ROCK family and have 89% homology of the kinase domain.<sup>23</sup> Both isoforms of ROCK consist of an N-

terminus kinase domain, which includes the activation loop and threonine phosphorylation site (Figure 1-4). Following the kinase domain is the coiled coil region that contains the Rho-binding domain.<sup>24</sup> This induces activation when Rho-GTP is bound. The structure of ROCK also includes a pleckstrin homology domain that contains a cysteine rich region.

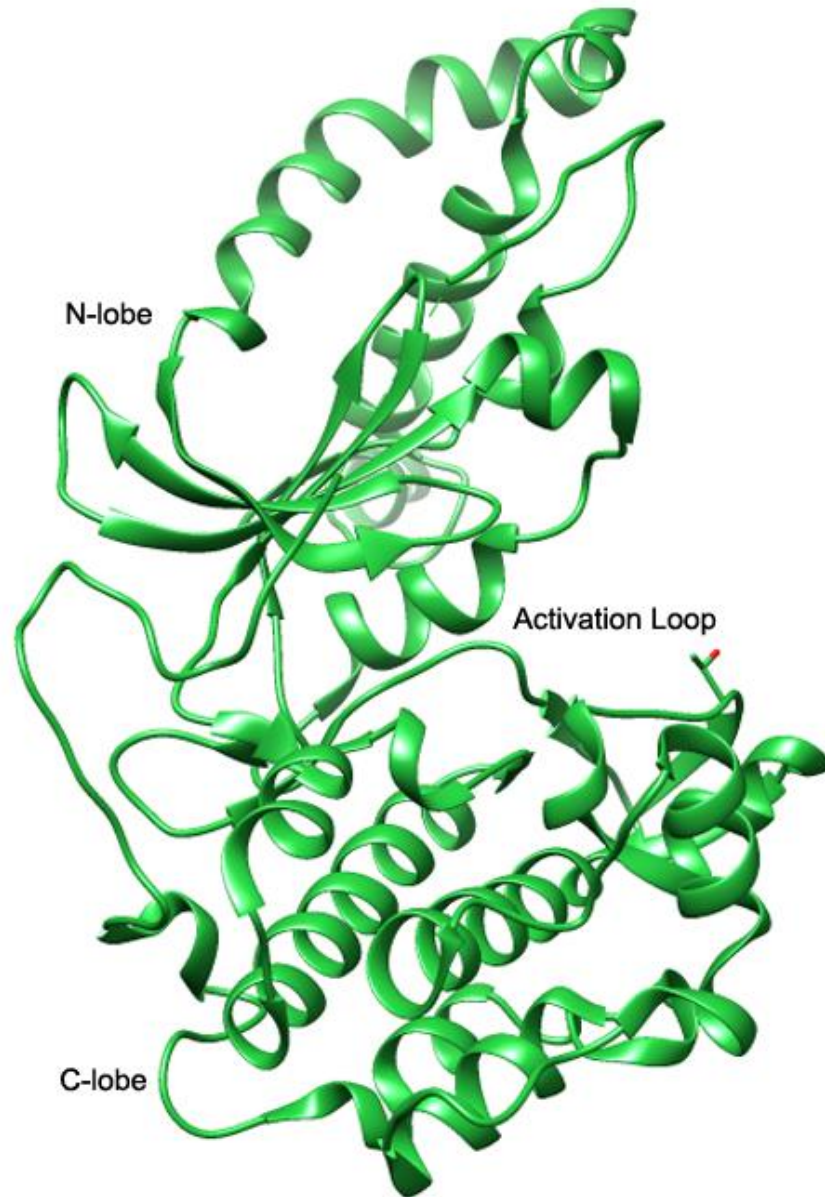


**Figure 1-4.** Kinase domain of ROCK2 with labelled activation loop and T240 phosphorylation site shown.<sup>25,26</sup>

ROCK is able to induce cell motility through the phosphorylation of multiple downstream targets. ROCK phosphorylates the regulatory subunit of the myosin light chain (MLC) and deactivates myosin-binding subunit of myosin light chain phosphatase.<sup>27</sup> This in turn leads to increased actomyosin-based contractility. ROCK also phosphorylates LIM kinases, including LIMK1, which leads to actin filament stabilization.<sup>28</sup> Through these three pathways, ROCK utilizes phosphorylation to activate downstream targets in order to induce cell motility (Figure 1-5).

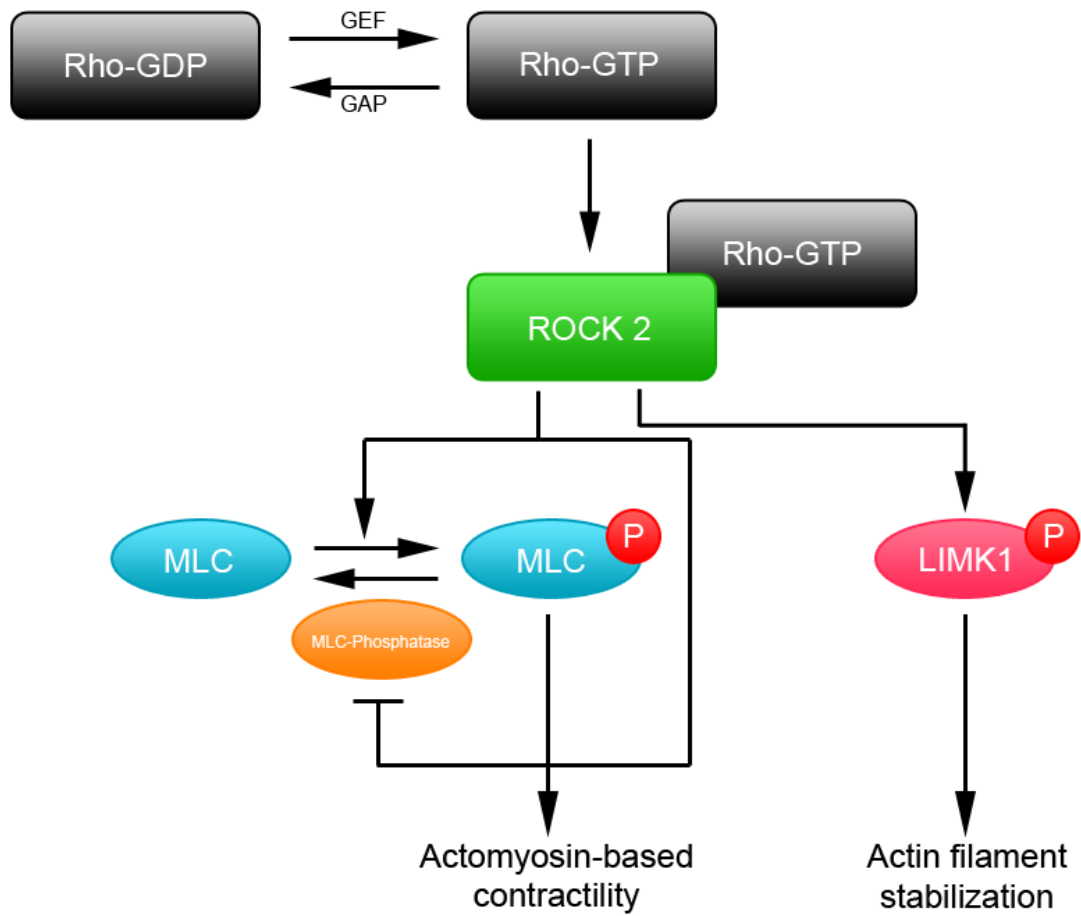


**Figure 1-5.** The pathway of ROCK2 that leads to productive cell motility through both actomyosin-based contractility and actin filament stabilization.

### **1.5 The need for a ROCK probe**

Beyond inhibitors, there is also a general need for a ROCK activity sensor. Current means of assessing ROCK activity fall short for the direct and continuous measurement. ROCK is activated through the binding of Rho-GTP and a conformational change to free the catalytic domain (Figure 1-6). The phosphorylation state of the kinase does not directly equate to the activity, therefore negating probing the phosphorylation state as a viable option for assessing the activity. Using a Western Blot to monitor the activity of ROCK in complex biological systems requires probing a downstream kinase's phosphorylation state. This method does not directly show ROCK activity, rather an indirect proxy for ROCK activity. There is a current need for a means to directly assess ROCK activity, such as with the direct and continuous CSox-based activity sensor.

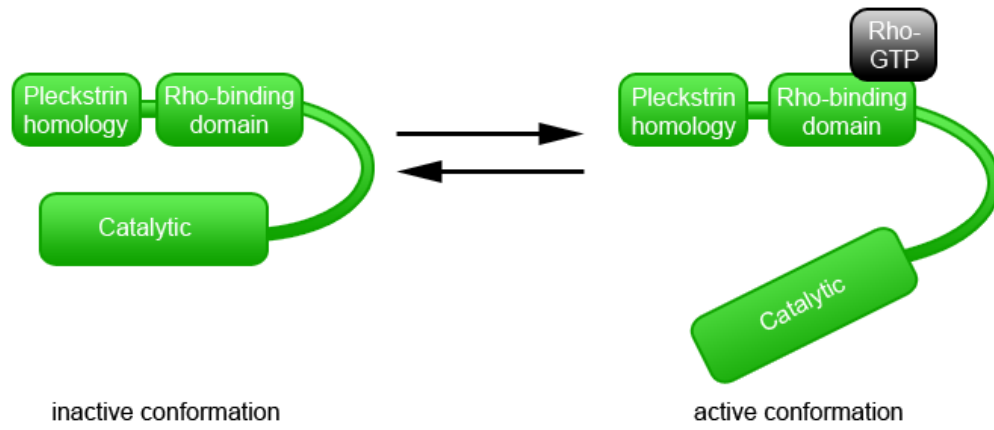


**Figure 1-6.** Rho-GTP binding induces a conformational change that activates ROCK2.

## **Chapter 2 – Design and Optimization of CSox-Based Sensor for Rho-Associated Protein Kinase and Implementation in High Throughput Screening**

### **2.1 Introduction**

The entirety of this paper entitled “A real-time, fluorescence-based assay for Rho-associated protein kinase activity” is presented in Appendix A.

As previously discussed, there is a desperate need for an activity sensor that is capable of directly and continuously monitoring the activity of ROCK in HTS. The goal of this work is to design and optimize such a sensor and identify novel inhibitor compounds of ROCK.

## 2.2 Results and discussion

### 2.2.1 Rational design and characterization of preliminary ROCK activity probes

In order to design a CSox-based activity sensor for ROCK, we first sought to identify viable peptide substrates to build upon. The Katayama lab screened 136 peptide substrates against ROCK2 using a radiolabel assay to determine the ability of ROCK2 to phosphorylate the substrates. These peptide substrates are derived from multiple kinases, including LIMK1, MLC, and MBS of MLC phosphatase. From these substrates, we identified one that had a low  $K_M$  and minimal off target binding, R22. R22 was derived from LIMK1 with a  $K_M$  of 1.9  $\mu\text{M}$ .<sup>29</sup> From this information and the preliminary  $K_M$  from the peptide, we hypothesized that we would be able to design a Sox sensor that is highly sensitive with  $\mu\text{M}$  affinity.

Using the R22 sequence, we synthesized two CSox-based activity sensors with CSox in the +2 and -2 position from the site of phosphorylation. These were termed ROCK-S1 and ROCK-S2 (Table 2-1). Previous research has shown that varying the site of CSox can drastically alter the affinity of the sensor.<sup>11,30</sup> For positive controls, we also synthesized the same sensors, but with phospho-threonine at the site of phosphorylation instead of threonine, ROCK-P1 and ROCK-P2 (Table 2-1).

Name	Sequence	Mg <sup>2+</sup> K <sub>D</sub> (mM)
ROCK-S1	KPARKKRYTV-CS <sub>ox</sub> -GNPYWM	420
ROCK-P1	KPARKKRYpTV-CS <sub>ox</sub> -GNPYWM	17
ROCK-S2	KPARKK-CS <sub>ox</sub> -YTVVGNPYWM	66
ROCK-P2	KPARKK-CS <sub>ox</sub> -YpTVVGNPYWM	7.1

**Table 2-1.** Sequences of ROCK Activity probes and Mg<sup>2+</sup> K<sub>D</sub> values.

In order to determine the optimal  $Mg^{2+}$  concentrations for ROCK-S1 and ROCK-S2, we measured both the control and experimental sensors with varying concentrations of  $Mg^{2+}$ . We expect the control sequences to exhibit a stronger affinity for  $Mg^{2+}$  because of their phosphorylation state (Figure 2-1). However, it is of importance to quantify the differences in  $Mg^{2+}$  affinities between sequences in order to properly control the concentration of  $Mg^{2+}$ .<sup>31</sup> Previous work from our laboratory has shown that this optimization is extremely important because of the dramatic improvement in assay performance.<sup>30</sup> After determining the  $K_D$  of  $Mg^{2+}$  and the sensor, we measured the fold fluorescence increase of each pair of control/experimental sensors by varying both  $Mg^{2+}$  and ATP concentrations (Table 2-2). We were able to observe the maximal fluorescence enhancements with 0.1 mM ATP. Previous work has demonstrated that the  $K_M$  of ROCK2 for ATP is 1.4 $\mu$ M, indicating that 0.1mM ATP could be used for enzymatic essays without severely interfering with the rate of substrate phosphorylation.<sup>32</sup>

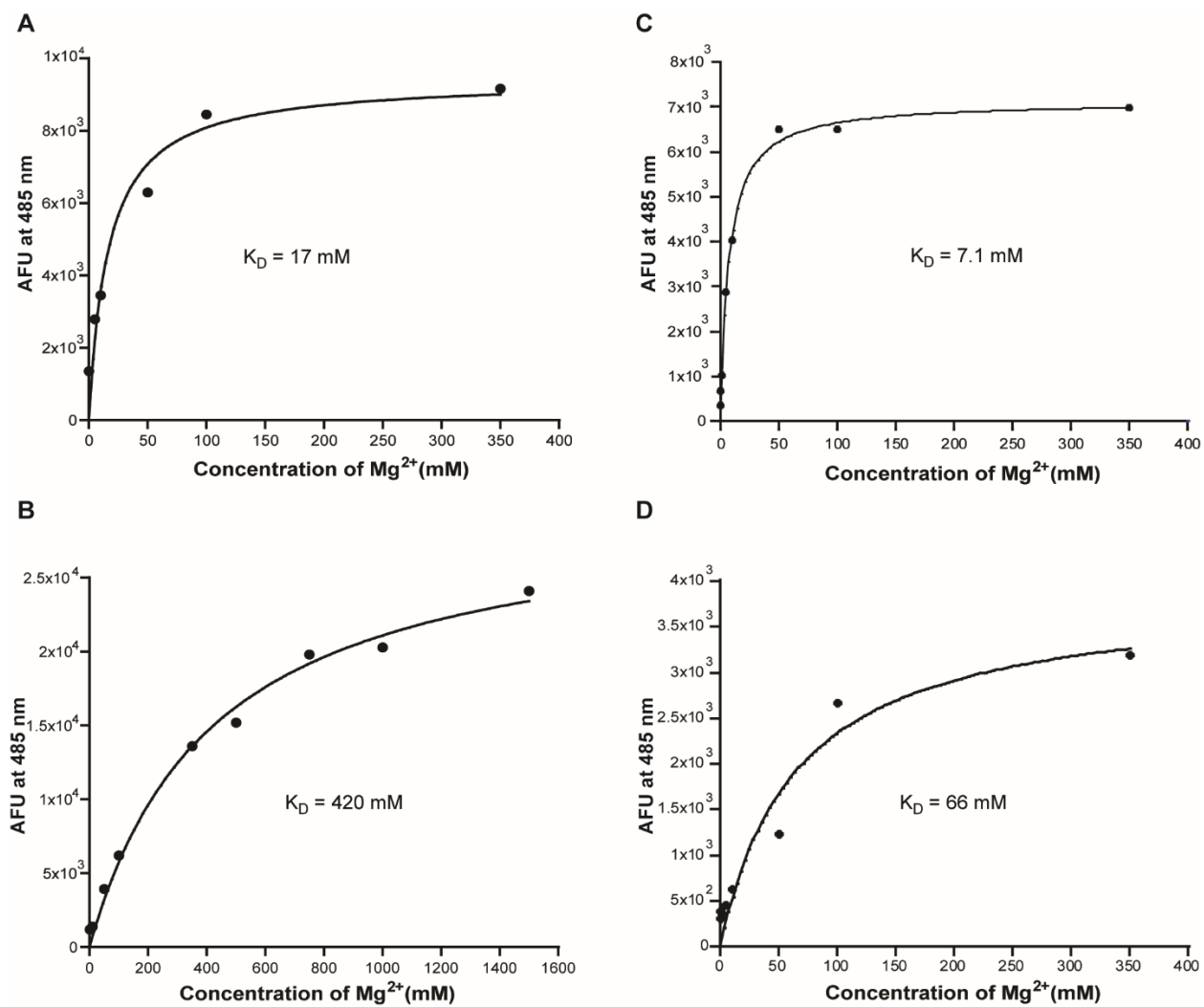


**Figure 2-1.** Fluorescence of ROCK-P1 (A), ROCK-S1 (B), ROCK-P2 (C), and ROCK-S2 (D) as a function of  $Mg^{2+}$  concentration.

Peptide	Mg <sup>2+</sup> (mM)	Fold Fluorescence Enhancements	
		0.1 mM ATP	1.0 mM ATP
ROCK-P1	10	2.7	2.1
	20	2.5	2.0
	40	2.0	1.8
ROCK-P2	3.5	4.9	3.5
	7.0	6.1	6.0
	10.5	7.0	6.5

**Table 2-2.** Fold fluorescence enhancements of ROCK-S1 and ROCK-S2 as a function of Mg<sup>2+</sup> and ATP concentrations. Fold fluorescence enhancement values were calculated by dividing the fluorescence of the phosphorylated positive control peptide by the fluorescence of the non-phosphorylated peptide.

### 2.2.2 Evaluation of probe efficiency for ROCK2

To establish the probe efficiency for ROCK2, we measured to rate of product formation with varied concentrations of each probe. These experiments were carried out using the optimal  $Mg^{2+}$  and ATP concentrations that were previously determined. In these experiments we observed substrate inhibition for both probes at increasing concentrations. This finding exemplifies why full characterization is needed for CSox-based activity probes. At  $>10 \mu M$  concentrations, the assay performance would be increasingly diminished. We were able to determine the  $K_M$ ,  $k_{cat}$  and  $k_{cat}/K_M$  from the assays which allowed us to determine the optimal sensor (Figure 2-2). By comparing the  $k_{cat}/K_M$  values for each probe, ROCK-S1 and ROCK-S2, we determined ROCK-S1 was 188-fold more efficient for ROCK2 (Table 2-3). ROCK-S2 has a 33 fold decrease in probe turnover by placing the CSox at the -2 position relative to the site of phosphorylation. Using the previous findings, we determined the optimal assay conditions and chose to employ ROCK-S1 at a concentration of  $5 \mu M$  for all subsequent experiments.

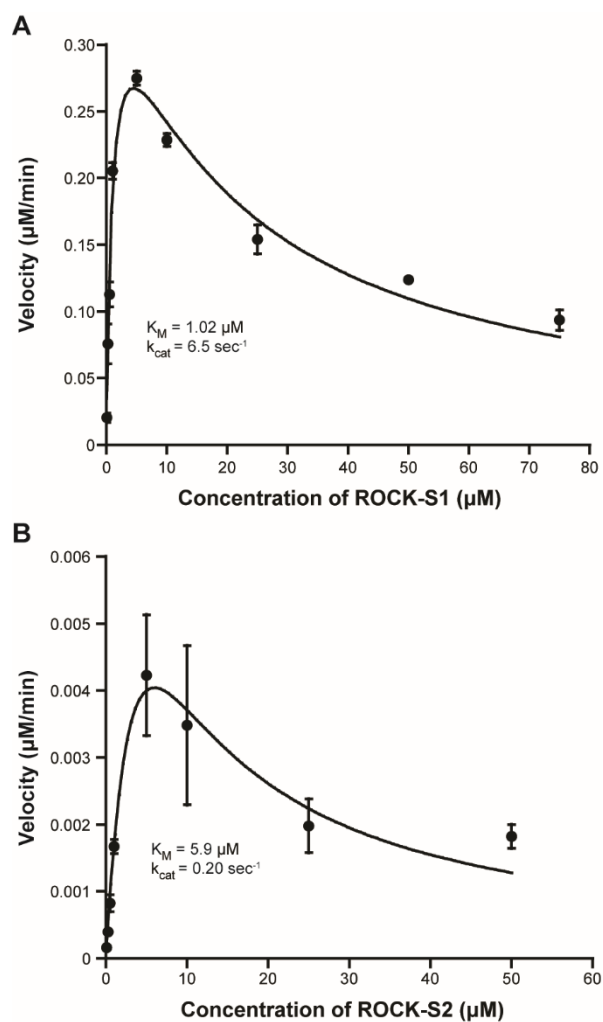


**Figure 2-2.** Kinetic parameters for ROCK-S1 (A) and ROCK-S2 (B) with ROCK2 (1 nM). Data was fit using Eq. 2.

Peptide	$k_{cat}/K_M$
ROCK-S1	$6.37 \times 10^6 \text{ M}^{-1} \text{ s}^{-1}$
ROCK-S2	$3.39 \times 10^4 \text{ M}^{-1} \text{ s}^{-1}$

**Table 2-3.**  $k_{cat}/K_M$  values for each sensor construct for the determination of the optimal sensor.

### 2.2.3 ROCK-S1 limit of detection for ROCK2

When optimizing a sensor, high sensitivity and high reproducibility of the sensor is ideal. This is especially important for assays that will be employed in HTS. We measured the phosphorylation of our probe, ROCK-S1, in the presence of decreasing amounts of ROCK2 to determine the sensitivity of the probe. Based on the data collected from these experiments, we calculated the limit of detection of ROCK-S1 with ROCK2 to be as low as 10 pM (Figure 2-3). This was determined based on the trend line,  $y = 701.7x - 4.1$  ( $R^2 = 0.9991$ ), where  $y$  is the average reaction slope in AFU/min and  $x$  is the concentration of ROCK2 in nM. These experiments were also determined to be highly reproducible ( $Z'$ -factor = 0.6 at 0.1 nM ROCK2), which further confirmed that these probes can be utilized in HTS. <sup>33</sup>

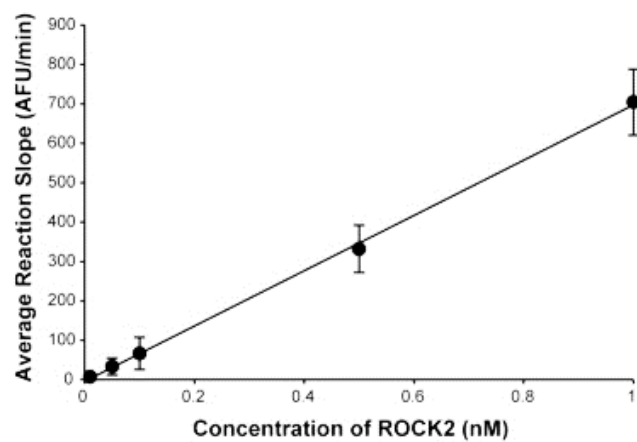


**Figure 2-3.** ROCK-S1 (5  $\mu\text{M}$ ) phosphorylation as a function of ROCK2 concentration.

#### **2.2.4 ROCK-S1 can report on ROCK2 inhibition**

We wanted to determine if ROCK-S1 could monitor the inhibition of ROCK2 in the presence of a known and well characterized ATP-competitive inhibitor, GSK429286.<sup>34</sup> Our results showed a concentration dependent decrease in activity that is consistent with our expectations (Figure 2-4). Our experimental IC<sub>50</sub> was consistent with the literature reported IC<sub>50</sub> value of 63 nM.<sup>35</sup> These results indicate that ROCK-S1 is capable of directly monitoring ROCK2 inhibition in a HTS format using a 384-well plates.

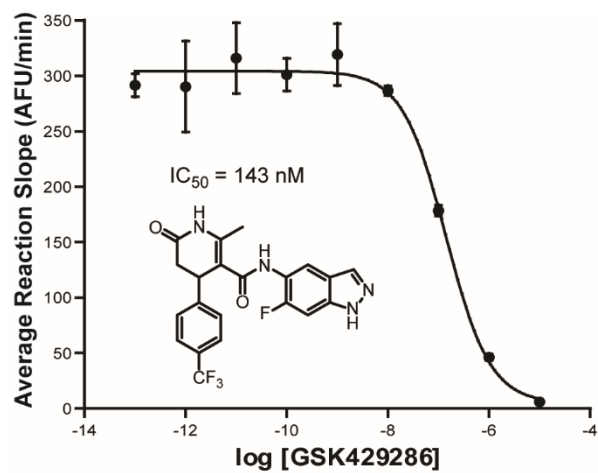


**Figure 2-4.** ROCK-S1 is able to monitor the inhibition of ROCK2 and produce results consistent with literature values.

### 2.2.5 Optimization of HTS conditions

Our goal was to implement our CSox-based activity sensor in a HTS to identify novel inhibitors of ROCK2. We chose a 78 compound library of known kinase inhibitors (Table 2-4). We expected six compounds to inhibit ROCK2 in this library. The five known ROCK2 inhibitors are fasudil<sup>36</sup>, Y27632<sup>37</sup>, HA1100<sup>38</sup>, H89<sup>30</sup>, and GW5074<sup>39</sup>, in addition to the broad spectrum inhibitor Ro318220.<sup>40</sup> To perform a high throughput screen, we used an automated robotics assay platform to monitor the inhibition of ROCK2 with ROCK-S1 with 10  $\mu$ M of each compound in quadruplicate 384-well plate assays. In addition to the five known inhibitors, we also observed >50% inhibition in the presence of two other inhibitors. PHA665752<sup>41</sup> and IKK16<sup>42</sup> have not been, to the best of our knowledge, identified as ROCK2 inhibitors in primary literature (Figure 2-5). To measure the effectiveness of each novel inhibitor, we obtained IC<sub>50</sub> value for both PHA665752 and IKK16 (Figure 2-6). We found that these novel inhibitors had low  $\mu$ M to high nM potency for ROCK2 in the presence of 0.1 mM ATP. Characterizing the known inhibitors of ROCK2 has the potential of eliminating off target inhibition. This off target activity has the potential to skew results, especially in cell-based assays that utilize high concentrations of inhibitors. In the future, these optimized condition could be used to screen a larger inhibitor library or fragment libraries for novel ROCK2 inhibitor scaffolds.

<b>Identifier</b>	<b>Inhibitor (10 <math>\mu</math>M)</b>	<b>% Inhibition</b>	<b>Std. Dev. (%)</b>
<b>A1</b>	GSK 429286	100	0.12
<b>A2</b>	ML 9	22	0.82
<b>A3</b>	NH 124	11	0.49
<b>A4</b>	Fasudil	66	0.39
<b>A5</b>	GF109203x	31	1.00
<b>A6</b>	Genistein	4	0.26
<b>A7</b>	LY294002	3	0.63
<b>A8</b>	U0126	3	0.33
<b>A9</b>	PD98059	3	0.30
<b>A10</b>	Y-27632	80	0.22
<b>B1</b>	No Inhibitor Control	-1	1.12
<b>B2</b>	Olomoucine	16	0.83
<b>B3</b>	LFM-A13	14	0.62
<b>B4</b>	ZM 336372	10	0.60
<b>B5</b>	ZM 449829	7	0.20
<b>B6</b>	ZM 39923	9	0.55
<b>B7</b>	GW 5074	52	2.26
<b>B8</b>	PP1	5	0.36
<b>B9</b>	SB 203580	12	0.18
<b>B10</b>	(-)-Tarreic acid	8	0.36
<b>C1</b>	PP 2	22	1.82

<b>C2</b>	SU 4312	21	1.25
<b>C3</b>	SP 600125	3	2.90
<b>C4</b>	Purvalanol A	13	0.49
<b>C5</b>	Purvanol B	16	0.47
<b>C6</b>	KU 55933	8	0.37
<b>C7</b>	AG 490	28	1.42
<b>C8</b>	SB 216763	8	0.58
<b>C9</b>	SB 415286	14	0.46
<b>C10</b>	Arctigenin	7	0.70
<b>D1</b>	NSC 693868	28	2.14
<b>D2</b>	SB 239063	21	1.24
<b>D3</b>	SL 327	21	1.70
<b>D4</b>	Ro 31-8220	55	0.97
<b>D5</b>	Aminopurvalanol A	21	1.29
<b>D6</b>	API-2	11	0.85
<b>D7</b>	GW 441756	17	1.38
<b>D8</b>	GW 583340	22	0.92
<b>D9</b>	Ro 08-2750	44	0.59
<b>D10</b>	TBB	11	0.09
<b>E1</b>	Hexabromocyclohexane	21	1.32
<b>E2</b>	HA 1100	68	0.37
<b>E3</b>	BIBX 1382	23	1.06
<b>E4</b>	CGP 53353	15	1.36

<b>E5</b>	Arcyriaflavin A	-9	1.02
<b>E6</b>	ZM 447439	20	0.86
<b>E7</b>	ER 27319	15	0.35
<b>E8</b>	ZM 323881	12	0.89
<b>E9</b>	ZM 306416	11	0.24
<b>E10</b>	IKK 16	81	0.87
<b>F1</b>	Ki 8751	24	1.39
<b>F2</b>	10-DEBC	21	0.79
<b>F3</b>	TPCA-1	22	0.53
<b>F4</b>	SB 218078	-26	6.40
<b>F5</b>	SB 202190	18	1.37
<b>F6</b>	PD 198306	13	0.67
<b>F7</b>	Ryuvidine	31	1.34
<b>F8</b>	IMD 0354	14	0.67
<b>F9</b>	CGK 733	11	0.20
<b>F10</b>	PHA 665752	85	0.85
<b>G1</b>	PD 407824	18	1.60
<b>G2</b>	LY 364974	17	1.08
<b>G3</b>	CGP 57380	16	1.21
<b>G4</b>	PQ 401	14	1.38
<b>G5</b>	PI 828	13	1.15
<b>G6</b>	NU 7026	12	0.90
<b>G7</b>	D4476	-23	5.10

<b>G8</b>	EO 1428	10	1.18
<b>G9</b>	H 89	76	1.28
<b>G10</b>	FPA 124	9	0.88
<b>H1</b>	GWn843682X	14	2.22
<b>H2</b>	Iressa	15	2.03
<b>H3</b>	SU 5416	10	1.73
<b>H4</b>	1-Naphthyl PP1	8	1.81
<b>H5</b>	GSK 650394	19	2.23
<b>H6</b>	BIO	5	1.66
<b>H7</b>	SD 208	11	1.10
<b>H8</b>	Compound 401	6	1.28
<b>H9</b>	BI 78D3	8	1.21
<b>H10</b>	SC 514	8	1.05

**Table 2-4.** Complete list of inhibitors in the library used for HTS.

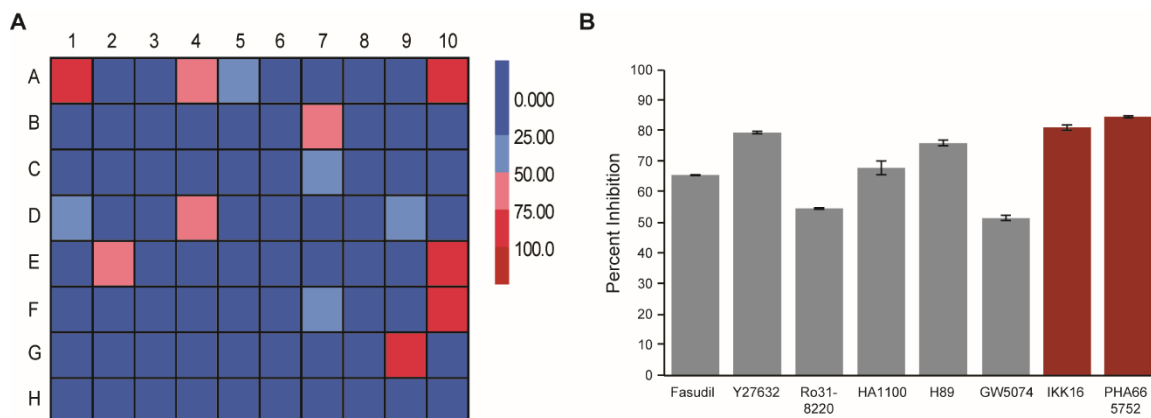


**Figure 2-5.** Proof-of-principle HTS for ROCK2 inhibitors. (A) compounds (10  $\mu$ M) were assayed against ROCK2 (1 nM) in the presence of 1 mM ATP. Percent inhibition was calculated from quadruplicate assays. A complete compound list is given in Table 2-4. Position A1 is 10  $\mu$ M GSK429286 and position B1 is no inhibitor. (B) Eight compounds displayed >50% ROCK2 inhibition. Six have been previously reported as ROCK2 inhibitors (grey bars) while three have not been previously reported to inhibit ROCK2 to the best of our knowledge (red bars).

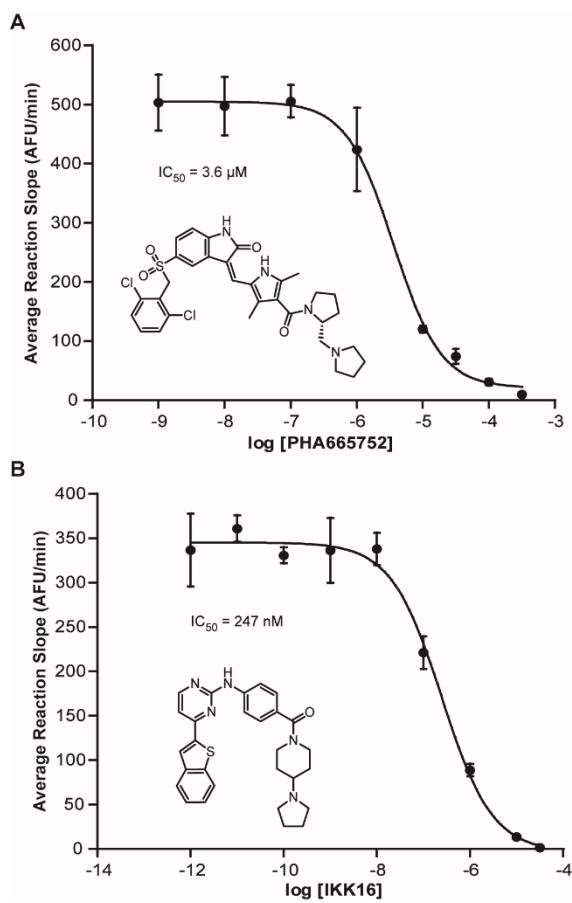


**Figure 2-6.** ROCK-S1 was used to monitor the inhibition of ROCK2 (5  $\mu\text{M}$ ) by PHA665752 and IKK16 (0.25 nM). Both inhibitors display low  $\mu\text{M}$  to high nM inhibition of ROCK2, respectively.

### 2.2.6 Selectivity of ROCK-S1

An important advantage that CSox-based activity sensors has over other current means of assessing kinase activity, is the ability to monitor the activity of a target kinase in complex biological samples, such as cell lysates and tissue homogenates.<sup>12,13,14,15</sup> In complex systems, there is the possibility of off-target activity on the sensor from other enzymes with similar consensus motifs. To remedy this, inhibitors for the off-target enzymes have been used to reduce the potential false positive signal in CSox-based assays.<sup>43,44,31,14</sup> Based on consensus motifs, we identified potential kinases that might present off target activity in complex biological systems.<sup>45,46</sup> We monitored the activity of ROCK2, ROCK1, PKC $\alpha$ , PKA, and PAK with ROCK-S1. The results indicated ROCK-S1 is phosphorylated by two off target enzymes from this panel, PKA and PKC $\alpha$  (Figure 2-7).

Based on this information, we wanted to determine if PKA and PKC $\alpha$  activity could be inhibited while maintaining ROCK activity. To accomplish this, we identified well-characterized PKA and PKC $\alpha$  inhibitors to utilize, including PKItide, PKC inhibitor peptide, calmidazolium and GF109203X.<sup>43</sup> Using the inhibitor cocktail described, we were able to preserve 58% of the activity of ROCK2 (Figure 2-8). Our panel does not contain all off-target enzyme possibilities in cell lysates, however; this work is a good first step in determining conditions for the analysis of ROCK activity *in vitro*.

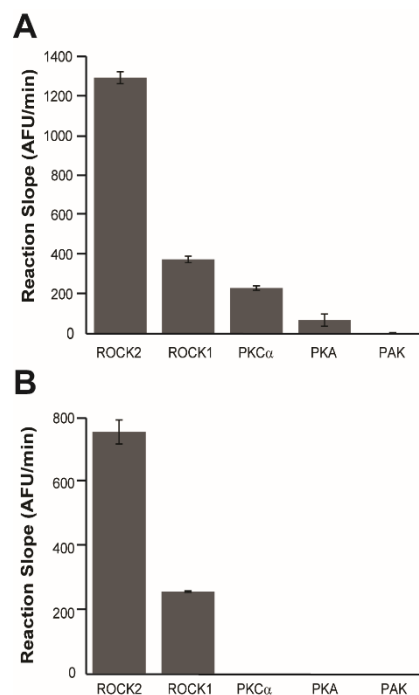


**Figure 2-7.** Selectivity for ROCK-S1. (A) The phosphorylation of ROCK-S1 (5  $\mu$ M) in the presence of the indicated enzyme (10 nM). (B) The same as panel A except the off-target inhibitors PKItide (0.4  $\mu$ M), PKC inhibitor peptide (4  $\mu$ M), GF109203X (5  $\mu$ M), and calmidazolium (4  $\mu$ M) are included.

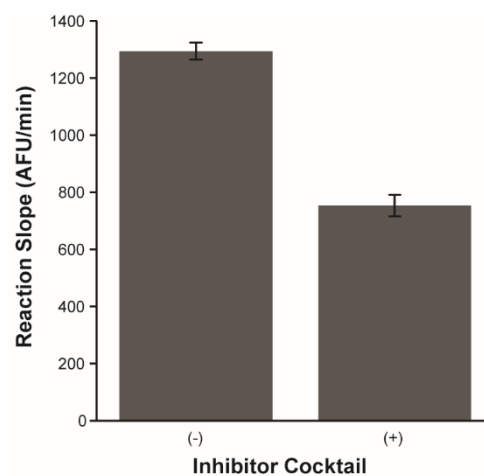


**Figure 2-8.** A significant proportion (58%) of ROCK2 activity is retained in the presence (+) of the inhibitor cocktail (0.4  $\mu$ M PKItide, 4  $\mu$ M PKC inhibitor peptide, 5  $\mu$ M GF109203X, and 4  $\mu$ M calmidazolium) compared to reactions performed without inhibitors (-).

## **2.3 Experimental**

### **2.3.1 General reagents, instrumentation, and procedures**

Fluorescence assays were conducted using a BioTek SynergyH2 microplate reader.

Assays were excited at 360 nm and the emission was recorded at 485 nm. Reactions were incubated at 30° C during fluorescence analysis. The plates used for fluorescence assays were either 384-well or 96-well half area plates (Corning: 3824 or 3992 respectively).

The total volume for assays was 40  $\mu$ L (384-well plates) or 120  $\mu$ L (96-well plates). All assays were conducted in triplicate unless otherwise noted.

### **2.3.2 Peptide synthesis**

Peptides were synthesized as previously described.<sup>31</sup> The peptides were purified using preparative reverse-phase HPLC and peptide identity was confirmed using ESI-MS (Table 2-5). To determine peptide concentration, the absorbance of each construct was measured and concentrations were calculated using the molar absorptivity of Sox, 8247  $M^{-1} cm^{-1}$  at 355 nm in 1 mM  $Na_2EDTA$  and 0.1 M  $NaOH$ .<sup>8</sup>

	Calculated Mass	Observed Mass
Peptide	$[M+xH]^{x+}$	$[M+xH]^{x+}$
<b>ROCK-S1</b>	$[M+2H]^{2+}$ : 1202.9	1202.7
<b>ROCK-P1</b>	$[M+2H]^{2+}$ : 1243.0	1243.5
<b>ROCK-S2</b>	$[M+2H]^{2+}$ : 1173.6	1173.9
<b>ROCK-P2</b>	$[M+2H]^{2+}$ : 1213.5	1213.9

**Table 2-5.** ESI-MS data for ROCK sensors.

### 2.3.3 Determination of $Mg^{2+}$ affinity and fold fluorescence increase

Stock solutions of  $Mg^{2+}$  were prepared from Alfa Aesar Puratronic grade  $MgCl_2$  salt and standardized by titration with EDTA in the presence of Eriochrome Black T. The  $Mg^{2+}$   $K_D$  was determined by measuring the fluorescence of each construct in the presence of 0.5, 1, 5, 10, 50, and 75 mM  $MgCl_2$  in a buffer containing 50 mM Tris-HCl (pH = 7.5 at 22° C) and 150 mM NaCl. Peptide was added to each assay at a final concentration of 1 mM. Fluorescence intensity was plotted and fit to a single site binding isotherm using Kaleidagraph to determine the  $K_D$  by fitting to Eq. (1).

$$emission\ at\ 485nm = (B_{max} * [Mg^{2+}]) / (K_D + [Mg^{2+}]) \quad (1)$$

Where  $B_{max}$  is the maximum specific binding in arbitrary fluorescence units and  $[Mg^{2+}]$  is the concentration of  $Mg^{2+}$  in mM.

The fold fluorescence increase of phospho- versus nonphosphosensors was performed for each set of peptides. The  $Mg^{2+}$  concentrations used for each set of constructs were chosen based on the  $K_D$  of the corresponding phospho-peptide. For each concentration of  $Mg^{2+}$ , two concentrations of ATP were investigated (0.1 mM and 1 mM).

### 2.3.4 Recombinant enzyme assays

Recombinant ROCK2 (Life Technologies, PV3759), was diluted in enzyme dilution buffer: 50 mM Tris-HCl (pH = 7.5 at 22°C), 1 mM EGTA, 0.01% Brij (v/v), and 10% glycerol (v/v). Kinase assays were conducted in a buffer containing: 50 mM Tris-HCl (pH = 7.5 at 22° C), 0.1 mM ATP, 1 mM EGTA, 2 mM DTT, 0.01% Brij (v/v), and the optimal  $Mg^{2+}$  concentration for each sensor. Assays were equilibrated to 30° C for 20 min before the addition of recombinant enzyme. Reaction velocities were determined by correcting for the loss of substrate fluorescence as previously described.<sup>8</sup> Kinetic

parameters were determined by plotting reaction velocities as a function of substrate concentration and fitting to Eq. (2) in Kaleidagraph.<sup>47</sup>

$$velocity = (V_{max} * [S]) / (K_M + [S] + \left(\frac{[S]^2}{K_S}\right)) \quad (2)$$

Where  $V_{max}$  is the maximum velocity,  $[S]$  is the concentration of substrate in  $\mu\text{M}$ ,  $K_M$  is the Michaelis-Menten constant, and  $K_S$  is the dissociation constant for substrate inhibition.

The limit of detection for the assay was defined as the smallest concentration ROCK2 that produced a signal that was three standard deviations above assay noise level. Enzymes used in the panel assay were purchased through Life Technologies and diluted in enzyme dilution buffer. Where indicated the following inhibitor cocktail was added to the panel assays: PKItide (0.4 mM), PKC inhibitor peptide (4 mM), GF109203X (5 mM), and calmidazolium (4 mM).<sup>43</sup>

### 2.3.5 High-throughput screening

Inhibitors were purchased from Tocris (3514) and supplied at 10 mM in DMSO. Inhibitors were diluted with PBS to a working concentration of 1 mM prior to screening. HTS assays were conducted using a robotics platform to prepare quadruplicate wells containing 1 nM ROCK2, 5 mM ROCK-S1, 1 mM ATP, 10 mM  $\text{MgCl}_2$ , 50 mM Tris-HCl (pH = 7.5 at 22°C), 1 mM EGTA, 2 mM DTT, 0.01% Brij (v/v), and 10 mM of the indicated inhibitor. The final concentration of 10 mM inhibitor was chosen in order to identify potential weak inhibitors. Wells with 10 mM GSK429286, no inhibitor, or no inhibitor and no enzyme were used as controls. Assays were performed in 384-well plates. Reaction slopes for each inhibitor were averaged and percent inhibition was calculated by comparison to controls. Two compounds from the initial 80 compound

commercial library (TCS359 and SB431542) are not included in the final data analysis due to extremely high autofluorescence, at a concentration of 10 mM, which resulted in detector overload. We did not observe any effect from DMSO on the rate of phosphorylation in these assays. Reaction slopes were determined using the initial linear regions of fluorescence data; fits contained at least 15 points.

## **2.4 Conclusions and Future Directions**

This work has focused on the design and optimization of a CSox-based ROCK sensor that can be utilized in HTS for novel inhibitor discovery. We have shown that this probe is capable of directly monitoring ROCK2 activity as well as ROCK2 inhibition. Through the work with HTS in a 384-well plate format using an automated robotics system, we have established the feasibility of implementing this system with larger inhibitor libraries. We have also begun to establish the optimal conditions for monitoring ROCK2 monitoring in complex biological systems through the utilization of an inhibitor cocktail that retains ROCK activity. In the future, ROCK-S1 will be employed to identify novel inhibitors of ROCK and interrogate ROCK activity perturbations in HCC.

## Appendix A

### A real-time, fluorescence-based assay for Rho-associated protein kinase activity

Reproduced with permission from:

M.I. Kelly, T.J. Bechtel, D.R. Reddy, E.D. Hankore, J.R. Beck, C.I. Stains. A real-time, fluorescence-based assay for Rho-associated protein kinase activity. *Anal. Chim. Acta.*

**891**, 284-290. (2015)

(doi: 10.1016/j.aca.2015.07.058)

Copyright 2015 Elsevier B.V.



Contents lists available at ScienceDirect

Analytica Chimica Acta

journal homepage: [www.elsevier.com/locate/aca](http://www.elsevier.com/locate/aca)

## A real-time, fluorescence-based assay for Rho-associated protein kinase activity



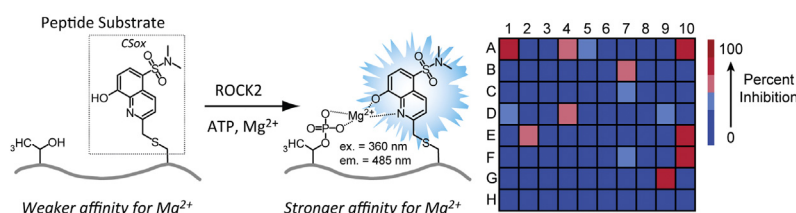
Maia I. Kelly<sup>3</sup>, Tyler J. Bechtel<sup>3,1</sup>, D. Rajasekhar Reddy<sup>2</sup>, Erome D. Hankore, Jon R. Beck, Cliff I. Stains\*

Department of Chemistry, University of Nebraska – Lincoln, Lincoln, NE 68588, United States

### HIGHLIGHTS

- Present a novel direct activity probe for ROCK.
- Demonstrate a limit of detection of 10 pM ROCK2.
- Demonstrate the ability to screen small molecules for ROCK2 inhibitors.
- Identify two previously unreported ROCK2 inhibitors.
- Provide conditions to selectively monitor ROCK activity.

### GRAPHICAL ABSTRACT



### ARTICLE INFO

#### Article history:

Received 23 May 2015

Received in revised form

28 July 2015

Accepted 31 July 2015

Available online 12 August 2015

#### Keywords:

Kinase activity assay

Fluorescence-based biosensor

Rho-associated protein kinase

Inhibition

Small molecule screening

### ABSTRACT

Inhibitors of Rho-associated protein kinase (ROCK) enzymatic activity have been shown to reduce the invasive phenotype observed in metastatic hepatocellular carcinoma (HCC). We describe the design, synthesis, and evaluation of a direct probe for ROCK activity utilizing a phosphorylation-sensitive sulfonamido-oxine fluorophore, termed Sox. The Sox fluorophore undergoes an increase in fluorescence upon phosphorylation of a proximal amino acid via chelation-enhanced fluorescence (CHEF, ex. = 360 nm and em. = 485 nm), allowing for the direct visualization of the rate of phosphate addition to a peptide substrate over time. Our optimal probe design, ROCK-S1, is capable of sensitively reporting ROCK activity with a limit of detection of 10 pM and a high degree of reproducibility ( $Z'$ -factor = 0.6 at 100 pM ROCK2). As a proof-of-principle for high-throughput screening (HTS) we demonstrate the ability to rapidly assess the efficacy of a 78 member, small molecule library against ROCK2 using a robotics platform. We identify two previously unreported ROCK2 inhibitor scaffolds, PHA665752 and IKK16, with IC<sub>50</sub> values of 3.6 μM and 247 nM respectively. Lastly, we define conditions for selectively monitoring ROCK activity in the presence of potential off-target enzymes (PKCα, PKA, and PAK) with similar substrate specificities.

© 2015 Elsevier B.V. All rights reserved.

**Abbreviations:** ROCK, rho-associated protein kinase; HCC, hepatocellular carcinoma; HTS, high-throughput screening; CHEF, chelation-enhanced fluorescence; Sox, sulfonamido-oxine; CSox, cysteine-Sox; DTT, dithiothreitol; EGTA, ethylene glycol tetraacetic acid; PBS, phosphate-buffered saline; K<sub>D</sub>, equilibrium dissociation constant.

\* Corresponding author.

E-mail address: [cstains2@unl.edu](mailto:cstains2@unl.edu) (C.I. Stains).

<sup>1</sup> Department of Chemistry, Boston College, Chestnut Hill, Massachusetts 02467, United States.

<sup>2</sup> Department of Biochemistry and Molecular Biophysics, Washington University School of Medicine, St. Louis, Missouri 63110, United States.

<sup>3</sup> These authors contributed equally to this work.

<http://dx.doi.org/10.1016/j.aca.2015.07.058>

0003-2670/© 2015 Elsevier B.V. All rights reserved.

## 1. Introduction

The five-year survival rate for HCC is 15% [1], due in large part to the aggressive nature of the disease when diagnosed in the clinic. As a consequence, significant efforts are needed to both enhance early detection and develop approaches for inhibiting the metastatic phenotype of HCC. Towards the latter goal, protein kinases represent attractive candidates for inhibitor development [2–4] and subsequent clinical intervention [5–8]. Previous work has shed light on the signaling molecules responsible for the invasive phenotype observed in HCC [9,10]. As a result of this work, ROCK has emerged as a potential target for inhibiting metastasis in HCC. ROCK1 and ROCK2 were originally identified as selective RhoA-GTP interacting proteins [11–13] and share 89% homology between their respective kinase domains [14]. ROCK couples Rho activation with contractile force generation through the direct phosphorylation of LIM kinases [15,16], the regulatory subunit of the myosin light chain [17,18], and the myosin-binding subunit of myosin light chain phosphatase [17]. Together these phosphorylation events lead to productive cell movement [19]. Interestingly, two HCC cell lines (Li7 and KYN-2) were found to have increased cell motility *in vitro* that could be blocked using C3 exoenzyme, a Rho inhibitor [9]. Stable transfection of a dominant negative form of ROCK into these cell lines also decreased cell motility and metastatic rate *in vivo* compared to the parent cell lines. In addition, a small molecule inhibitor of ROCK activity, Y27632 [20], significantly impaired the ability of Li7 cells to form metastatic nodules in mice [10]. Overall, this work adds to the growing evidence that ROCK activity is necessary for the metastatic phenotype observed in HCC and that ROCK inhibitors could provide a means for interfering with the progression of HCC in the clinic.

In general, current protein kinase activity assays rely on the use of radioactivity or high-cost reagents and/or instrumentation [21,22]. A variety of assay formats have been described that leverage the specificity and sensitivity of antibody-based reagents [23–25]. These techniques represent powerful approaches to monitoring kinase activity; however, the costs of these assay formats, and in certain cases the necessity of specialized equipment, can hinder their application in HTS. Alternatively, peptide-based kinase activity probes, capable of producing a change in fluorescence signal upon phosphorylation, can provide a straightforward, low-cost alternative for HTS [26–33]. As one example, the Imperiali laboratory has recently described the use of the phosphorylation-sensitive Sox fluorophore as a general platform for the design of sensitive serine/threonine and tyrosine kinase activity sensors [28,29,34,35]. These Sox probes detect phosphorylation of a proximal residue through CHEF upon binding of  $Mg^{2+}$ . However, initial Sox-based probe designs required deletion of sequences either N- or C-terminal to the phosphorylation site in order to install a  $\beta$ -turn to allow for productive CHEF. To address this issue, a second generation probe design was envisioned in which a cysteine derivative, termed CSox, could be substituted for a native amino acid proximal to the site of phosphorylation [36]. These second generation CSox-based sensors allow for productive CHEF while necessitating only a single amino acid substitution in a peptide substrate (Fig. 1). As a consequence, CSox-based probes display tighter  $K_M$  values for their target kinases, allowing for the use of reduced sensor concentrations in assays [37–40]. CSox-based probes for protein kinase activity can be rapidly constructed using standard solid-phase peptide synthesis and can provide a direct, real-time readout of kinase enzymatic activity [41]. Moreover, the Dalby laboratory has recently demonstrated the use of CSox-based probes to identify inhibitors of eEF-2 from a HTS screen using 32,960 compounds [30]. This work demonstrates that CSox-based probes can reduce the false positive rate associated with autofluorescence of inhibitors in

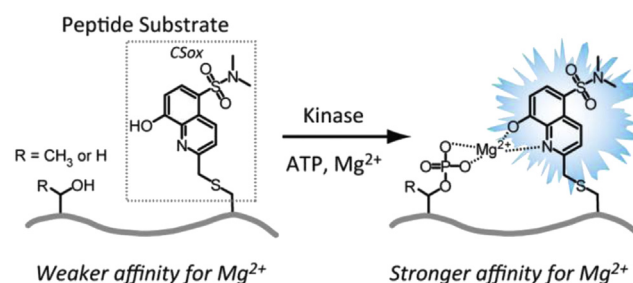


**Fig. 1.** A single amino acid in a peptide substrate is replaced with CSox (left). Phosphorylation of an adjacent amino acid leads to CHEF, which can be quantified by excitation at 360 nm and monitoring emission at 485 nm (right). The increase in fluorescence over time is proportional to kinase enzymatic activity.

HTS, since fluorescence changes are monitored over time as opposed to endpoint assays. The goal of the current work was to determine whether CSox could be employed to construct a sensitive and robust sensor for ROCK enzymatic activity, with the long term goal of utilizing this probe to discover novel ROCK inhibitors as well as interrogate ROCK activity in human disease states.

## 2. Experimental

### 2.1. General reagents, instrumentation, and procedures

Fluorescence assays were conducted using a BioTek SynergyH2 microplate reader. Assays were excited at 360 nm and the emission was recorded at 485 nm. Reactions were incubated at 30 °C during fluorescence analysis. The plates used for fluorescence assays were either 384-well or 96-well half area plates (Corning: 3824 or 3992 respectively). The total volume for assays was 40  $\mu$ L (384-well plates) or 120  $\mu$ L (96-well plates). All assays were conducted in triplicate unless otherwise noted.

### 2.2. Peptide synthesis

Peptides were synthesized as previously described [41]. The peptides were purified using preparative reverse-phase HPLC and peptide identity was confirmed using ESI-MS (Table S1). To determine peptide concentration, the absorbance of each construct was measured and concentrations were calculated using the molar absorptivity of Sox, 8247  $M^{-1} cm^{-1}$  at 355 nm in 1 mM  $Na_2EDTA$  and 0.1 M NaOH [34].

### 2.3. Determination of $Mg^{2+}$ affinity and fold fluorescence increase

Stock solutions of  $Mg^{2+}$  were prepared from Alfa Aesar Pura-tronic grade  $MgCl_2$  salt and standardized by titration with EDTA in the presence of Eriochrome Black T. The  $Mg^{2+}$   $K_D$  was determined by measuring the fluorescence of each construct in the presence of 0.5, 1, 5, 10, 50, and 75 mM  $MgCl_2$  in a buffer containing 50 mM Tris-HCl (pH = 7.5 at 22 °C) and 150 mM NaCl. Peptide was added to each assay at a final concentration of 1  $\mu$ M. Fluorescence intensity was plotted and fit to a single site binding isotherm using Kaleidagraph to determine the  $K_D$  by fitting to Eq. (1).

$$\text{emission at } 485 \text{ nm} = \left( B_{\max} * [Mg^{2+}] \right) / \left( K_D + [Mg^{2+}] \right) \quad (1)$$

where  $B_{\max}$  is the maximum specific binding in arbitrary fluorescence units and  $[Mg^{2+}]$  is the concentration of  $Mg^{2+}$ .

The fold fluorescence increase of phospho- versus nonphospho-sensors was performed for each set of peptides. The  $Mg^{2+}$

concentrations used for each set of constructs were chosen based on the  $K_D$  of the corresponding phospho-peptide. For each concentration of  $Mg^{2+}$ , two concentrations of ATP were investigated (0.1 mM and 1 mM).

#### 2.4. Recombinant enzyme assays

Recombinant ROCK2 (Life Technologies, PV3759), was diluted in enzyme dilution buffer: 50 mM Tris–HCl (pH = 7.5 at 22 °C), 1 mM EGTA, 0.01% Brij (v/v), and 10% glycerol (v/v). Kinase assays were conducted in a buffer containing: 50 mM Tris–HCl (pH = 7.5 at 22 °C), 0.1 mM ATP, 1 mM EGTA, 2 mM DTT, 0.01% Brij (v/v), and the optimal  $Mg^{2+}$  concentration for each sensor. Assays were equilibrated to 30 °C for 20 min before the addition of recombinant enzyme. Reaction velocities were determined by correcting for the loss of substrate fluorescence as previously described [34]. Kinetic parameters were determined by plotting reaction velocities as a function of substrate concentration and fitting to Eq. (2) in Kaleidagraph [42].

$$\text{velocity} = (V_{\max} * [S]) / (K_M + [S] + ([S]^2 / K_S)) \quad (2)$$

where  $V_{\max}$  is the maximum velocity,  $[S]$  is the concentration of substrate,  $K_M$  is the Michaelis–Menten constant, and  $K_S$  is the dissociation constant for substrate inhibition. The limit of detection for the assay was defined as the smallest concentration ROCK2 that produced a signal that was three standard deviations above assay noise.

Enzymes used in the panel assay were purchased through Life Technologies and diluted in enzyme dilution buffer. Where indicated the following inhibitor cocktail was added to the panel assays: PKItide (0.4  $\mu$ M), PKC inhibitor peptide (4  $\mu$ M), GF109203X (5  $\mu$ M), and calmidazolium (4  $\mu$ M) [35].

#### 2.5. High-throughput screening

Inhibitors were purchased from Tocris (3514) and supplied at 10 mM in DMSO. Inhibitors were diluted with PBS to a working concentration of 1 mM prior to screening. HTS assays were conducted using a robotics platform to prepare quadruplicate wells containing 1 nM ROCK2, 5  $\mu$ M ROCK-S1, 1 mM ATP, 10 mM  $MgCl_2$ , 50 mM Tris–HCl (pH = 7.5 at 22 °C), 1 mM EGTA, 2 mM DTT, 0.01% Brij (v/v), and 10  $\mu$ M of the indicated inhibitor. The final concentration of 10  $\mu$ M inhibitor was chosen in order to identify potential weak inhibitors. Wells with 10  $\mu$ M GSK429286, no inhibitor, or no inhibitor and no enzyme were used as controls. Assays were performed in 384-well plates. Reaction slopes for each inhibitor were averaged and percent inhibition was calculated by comparison to controls. Two compounds from the initial 80 compound commercial library (TCS359 and SB431542) are not included in the final data analysis due to extremely high autofluorescence, at a concentration of 10  $\mu$ M, which resulted in detector overload. We did not observe any effect from DMSO on the rate of phosphorylation in these assays. Reaction slopes were determined using the initial linear regions of fluorescence data; fits contained at least 15 points.

### 3. Results and discussion

#### 3.1. Rational design and characterization of preliminary ROCK activity probes

As a first step towards the development of a CSox-based ROCK activity sensor we set out to identify optimal peptide substrates for ROCK. Recent work from the Katayama laboratory has examined the ability of ROCK2 to phosphorylate a library of 136 peptides [43].

From this work, a sequence dubbed R22 was identified with a  $K_M$  of 1.9  $\mu$ M. We hypothesized that this sequence could be employed to generate a CSox-based chemosensor with low  $\mu$ M affinity for ROCK2 in order to allow for minimal sensor usage during HTS. Accordingly, we synthesized two CSox-based activity probes using R22 as the template sequence with CSox placed at the +2 and –2 positions relative to the site of phosphorylation, ROCK-S1 and ROCK-S2 (Table 1). These two probe sequences represent important steps in sensor optimization, as previous work has demonstrated that the positioning of CSox in a peptide substrate sequence can dramatically alter the sensitivity of probe constructs [36,40]. In addition, we synthesized the corresponding positive control sequences containing phospho-threonine at the site of phosphorylation, ROCK-P1 and ROCK-P2 (Table 1).

Next, we measured the affinity of each peptide construct for  $Mg^{2+}$  (Fig. S1). Although positive control (phosphorylated) sequences are expected to display stronger affinities for  $Mg^{2+}$ , it is important to quantify the difference in affinities of substrate and product sequences such that  $Mg^{2+}$  concentrations can be appropriately controlled for each construct [41]. Indeed, previous work from our laboratory has demonstrated that this optimization step can provide a dramatic enhancement in assay performance [40]. Using these experimentally determined  $Mg^{2+}$  affinities as a guide (Table 1), we measured the increase in fluorescence of each pair of product versus substrate peptides under varying  $Mg^{2+}$  and ATP concentrations (Table S2). Under optimized conditions, using 0.1 mM ATP, we were able to obtain robust enhancements in probe fluorescence in response to phosphorylation (Table 1). Importantly, previous work has demonstrated that the  $K_M$  of ROCK2 for ATP is 1.4  $\mu$ M [44], indicating that 0.1 mM ATP could be used for enzymatic assays without severely interfering with the rate of substrate phosphorylation.

#### 3.2. Evaluation of probe efficiency for ROCK2

Using the optimized  $Mg^{2+}$  and ATP concentrations identified above, we interrogated the preference of ROCK2 for the position of CSox within our probe sequences. Accordingly, we varied the concentration of each substrate and measured the resulting rate of product formation (Fig. 2). Interestingly, we observed substrate inhibition for each probe design at increasing sensor concentrations. These results highlight the importance of fully characterizing CSox-based activity probes, as the use of higher concentrations (>10  $\mu$ M) of the sensors described in this paper would lead to diminished assay performance. Comparison of  $k_{\text{cat}}/K_M$  for each sensor design indicated that ROCK-S1 was 188-fold more efficient for ROCK2. In particular, we observed a 33-fold decrease in probe turnover by positioning CSox at the –2 position relative to the site of phosphorylation in ROCK-S2. This indicates the sensitivity of ROCK2 to CSox at this position. Using these experimental results as a guide, we chose to employ ROCK-S1 at a concentration of 5  $\mu$ M for all subsequent experiments.

#### 3.3. ROCK-S1 limit of detection for ROCK2

One significant source of cost during HTS is recombinant kinase. As a consequence, assays with low detection limits and high reproducibility are desirable. To determine the sensitivity of ROCK-S1, we measured sensor phosphorylation in the presence of decreasing amounts of ROCK2. These experiments indicated the ability to detect ROCK2 activity at concentrations as low as 10 pM (Fig. 3). The trend line for this data is  $y = 701.7x - 4.1$  ( $R^2 = 0.9991$ ), where  $y$  is the average reaction slope in AFU/min and  $x$  is the concentration of ROCK2 in nM. Moreover, these assays were highly reproducible ( $Z'$ -factor = 0.6 at 0.1 nM ROCK2), validating the use of ROCK-S1 for HTS [45].

**Table 1**  
Sequences of ROCK activity probes.

Name	Sequence <sup>a</sup>	Mg <sup>2+</sup> K <sub>D</sub> (mM)	Fold Fluorescence Enhancement <sup>b</sup>
ROCK-S1	KPARKKRYTV- <b>CSox</b> -GNPYWM	420	
ROCK-P1	KPARKKRY <b>p</b> TV- <b>CSox</b> -GNPYWM	17	2.7
ROCK-S2	KPARKK- <b>CSox</b> -YTVVGNPYWM	66	
ROCK-P2	KPARKK- <b>CSox</b> -Y <b>p</b> TVVGNPYWM	7.1	7.0

<sup>a</sup>The site of phosphorylation is shown in red and the position of CSox is highlighted in blue.

<sup>b</sup>Fold fluorescence enhancements are obtained by dividing the fluorescence of the phosphorylated peptide by the fluorescence of the corresponding nonphosphorylated peptide. Assays were performed with 0.1 mM ATP and the optimal concentration of Mg<sup>2+</sup> for each sensor construct (10 and 10.5 mM Mg<sup>2+</sup> for ROCK-P1 and ROCK-P2 respectively).

### 3.4. ROCK-S1 can report on ROCK2 inhibition

As an initial test of whether ROCK-S1 could report on ROCK2 inhibition we assessed ROCK-S1 phosphorylation in the presence of increasing concentrations of GSK429286, a well-characterized ATP-competitive ROCK2 inhibitor [46]. As expected, we observed a

concentration dependent decrease in ROCK-S1 phosphorylation that correlated with the literature IC<sub>50</sub> value of 63 nM (Fig. 4) [47]. These data indicate the ability to straightforwardly monitor ROCK2 inhibition using ROCK-S1 in a 384-well format.

### 3.5. Optimization of HTS conditions

As a proof-of-principle for HTS using ROCK-S1 we chose to screen a commercially available 78 compound library of kinase

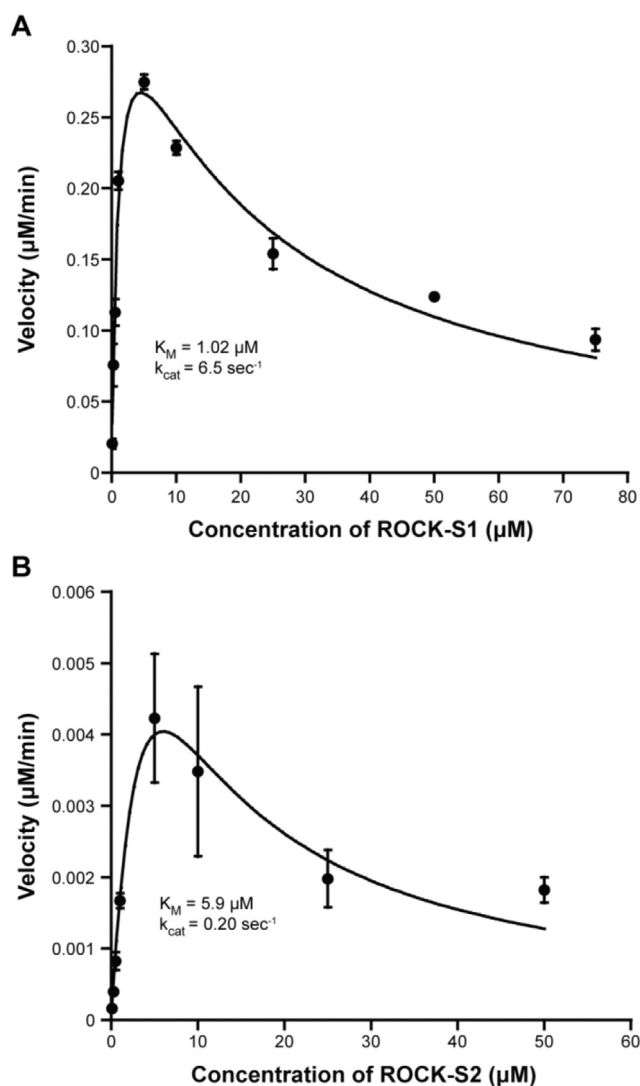


**Fig. 2.** Kinetic parameters for ROCK-S1 (A) and ROCK-S2 (B) with ROCK2 (1 nM). Data were fit by using a modified form of the Michaelis-Menten equation [42], given in the Experimental Section, in order to account for substrate inhibition.

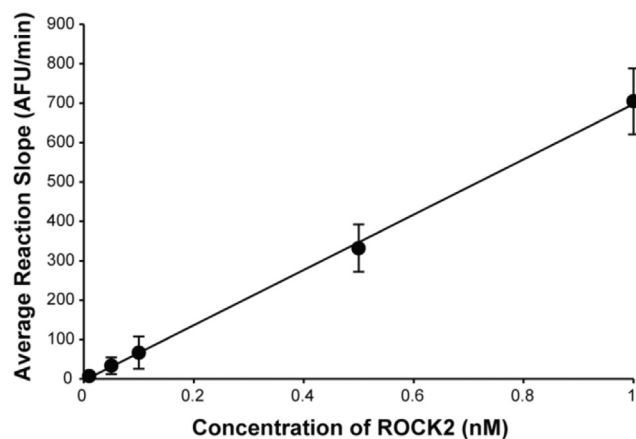


**Fig. 3.** ROCK-S1 (5  $\mu\text{M}$ ) phosphorylation as a function of ROCK2 concentration.

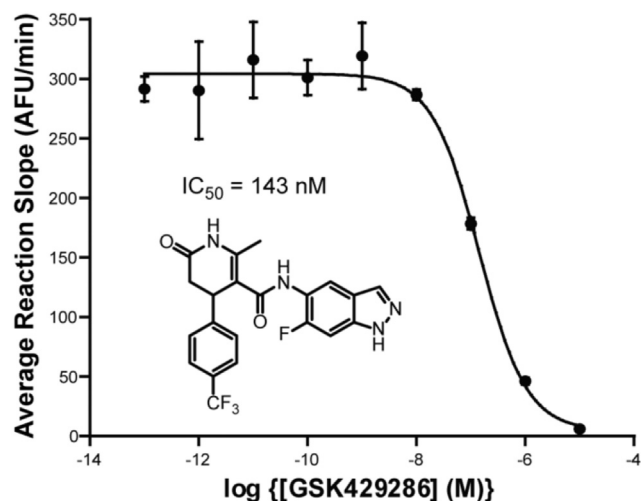


**Fig. 4.** ROCK-S1 (5  $\mu\text{M}$ ) can report on the inhibition of ROCK2 (0.5 nM) by a well-characterized ATP-competitive inhibitor.

inhibitors (Table S3). Importantly this library contains five known inhibitors of ROCK2; fasudil [48], Y27632 [20], HA1100 [49], H89 [50], and GW5074 [51] as well as the broad spectrum inhibitor Ro318220 [50]. Utilizing an automated robotics assay platform we assessed the percent inhibition of each compound in our library at a concentration of 10  $\mu\text{M}$  in quadruplicate 384-well plate assays (Fig. 5A). As expected, we observed >50% inhibition of ROCK2 by fasudil, Y27632, HA1100, H89, GW5074, and Ro318220 (Fig. 5B). Interestingly, we also observed >50% inhibition by two additional inhibitors (PHA665752 [52] and IKK16 [53]) that to the best of our knowledge have not been previously reported as ROCK2 inhibitors in the primary literature (Fig. 5B). To further investigate the potency of these inhibitors we obtained  $\text{IC}_{50}$  values for each of these scaffolds against ROCK2 (Fig. 6). Although these inhibitors displayed low  $\mu\text{M}$  to high nM potency for ROCK2 in the presence of 0.1 mM ATP, the relatively high concentrations of inhibitors generally used during cell-based assays may lead to off-target effects. As a consequence, the off-target effects of these inhibitors could have important ramifications for the interpretation of phenotypic assays. In the long term, the conditions outlined in this work could be used to screen larger compound or fragment libraries for novel ROCK2 inhibitor scaffolds.

### 3.6. Selectivity of ROCK-S1

Another significant advantage of CSox-based activity sensors is the ability to selectively report on the activity of protein kinases in heterogeneous biological samples such as cell lysates and tissue homogenates [37,38,54,55]. However, in these complex samples off-target activity can be observed from enzymes with overlapping sequence specificity. In these situations off-target inhibitors have been effectively employed to reduce potential false positive signal in CSox-based assays [35,39,41,54]. As a first step towards defining conditions for monitoring ROCK activity in heterogeneous samples we assessed the selectivity of ROCK-S1 across a panel of protein kinases including ROCK2, ROCK1, PKC $\alpha$ , PKA, and PAK. Importantly, previous data demonstrated that the peptide sequence that serves as a template for ROCK-S1 could act as a substrate for PKC $\alpha$ , PKA, and PAK [15,43]. Our data demonstrates that our CSox-based probe, ROCK-S1, could also be phosphorylated by PKA and PKC $\alpha$  (Fig. 7A). We next investigated whether PKA and PKC $\alpha$  activities could be suppressed with known inhibitors [35]. Accordingly we chose to employ well-characterized PKA and PKC $\alpha$  inhibitors: PKItide, PKC inhibitor peptide, calmidazolium, and GF109203X [35]. This inhibitor cocktail preserved a significant portion, 58%, of ROCK2

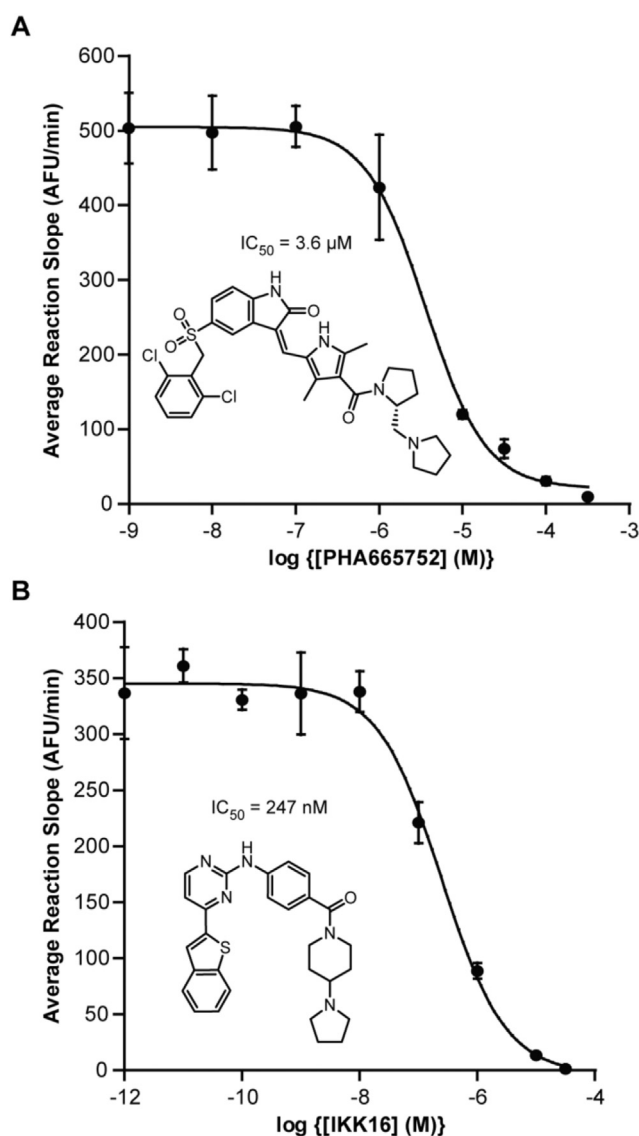


Fig. 6. The indicated inhibitors were assayed against ROCK2 (0.25 nM) and inhibition was monitored using ROCK-S1 (5  $\mu\text{M}$ ) in the presence of 0.1 mM ATP. Each scaffold displays low  $\mu\text{M}$  to high nM inhibition of ROCK2.

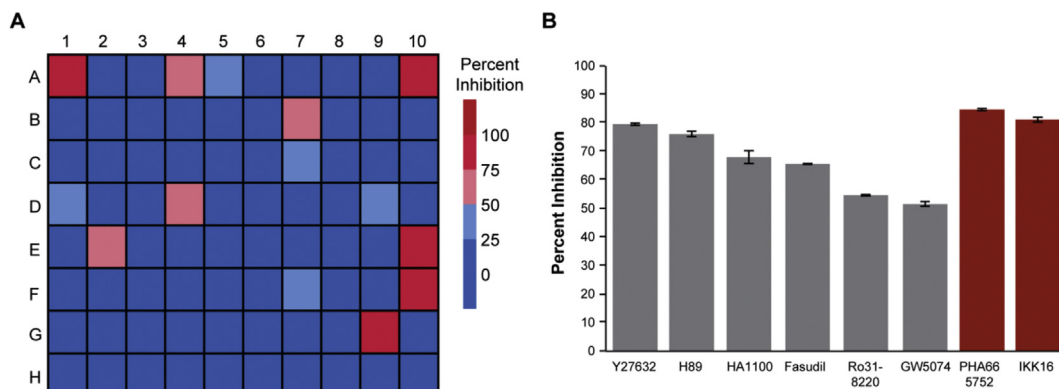


Fig. 5. Proof-of-principle HTS for ROCK2 inhibitors. (A) Compounds (10  $\mu\text{M}$ ) were assayed against ROCK2 (1 nM) in the presence of 1 mM ATP. Percent inhibition was calculated from quadruplicate assays. A complete compound list is given in Table S3. Position A1 corresponds to 10  $\mu\text{M}$  GSK429286 (positive control) and position B1 represents no inhibitor (negative control). (B) Eight compounds from the library displayed >50% ROCK2 inhibition. Six have been previously reported as ROCK2 inhibitors (grey bars) while two have, to the best of our knowledge, not been previously reported to inhibit ROCK2 (red bars). (For interpretation of the references to colour in this figure legend, the reader is referred to the web version of this article.)

activity (Fig. S2). However, the same inhibitor cocktail was capable of completely abolishing the off-target phosphorylation of ROCK-S1 (Fig. 7B). Although our panel does not contain every possible off-target enzyme present in cell lysates, this work represents an important first step towards defining conditions for the analysis of ROCK activity in complex biological samples such as cell lysates and tissue homogenates. Future experiments will be aimed at identifying optimized inhibitor cocktails that have a reduced effect on ROCK activity as well as accessing ROCK-S1 selectivity in cell lysates.

#### 4. Conclusions

Taken together, this work defines a new CSox-based probe along with optimized assay conditions for the direct analysis of ROCK2 activity. We have demonstrated the ability to utilize ROCK-S1 to rapidly screen inhibitor libraries in a 384-well plate format using an automated robotics system. This bioanalytical tool provides a straightforward approach to screening small molecule or fragment libraries for potential ROCK2 inhibitors. The ROCK2 inhibitor scaffolds identified in this study (PHA665752 and IKK16) could provide

a starting point for the development of ROCK2 inhibitors, although the target specificity of these scaffolds would certainly need to be optimized. In addition, we have defined conditions that allow for the selective monitoring of ROCK activity in the presence of potential off-target enzymes. The sensitivity of ROCK-S1, 10 pM ROCK2, is on par with previously described Sox-based probes that have been successfully utilized to detect kinase activity in unfractionated cell lysates [34,35,38,39,54]. Consequently, our laboratory is currently investigating the use of ROCK-S1 to identify novel inhibitors of ROCK as well as interrogate ROCK activity perturbations in HCC.

#### Acknowledgments

We acknowledge the Nebraska Center for Mass Spectrometry for assistance with peptide characterization and the HTS facility at the University of Nebraska Medical Center for assistance with proof-of-principle library screening. This work was funded by the Nebraska Research Initiative, the Proposed Center for Integrated Biomolecular Communication, the Fred & Pamela Buffett Cancer Center, and the Department of Chemistry at the University of Nebraska–Lincoln. T. J. Bechtel was supported by an NSF REU grant (1156560).

#### Appendix A. Supplementary data

Supplementary data related to this article can be found at <http://dx.doi.org/10.1016/j.aca.2015.07.058>.

#### References

- [1] R. Siegel, D. Naishadham, A. Jemal, *Cancer statistics, 2013*, *CA-Cancer J. Clin.* 63 (2013) 11–30.
- [2] R.S. Vidadala, K.K. Ojo, S.M. Johnson, Z. Zhang, S.E. Leonard, A. Mitra, R. Choi, M.C. Reid, K.R. Keyloun, A.M. Fox, M. Kennedy, T. Silver-Brace, J.C. Hume, S. Kappe, C.L. Verlinde, E. Fan, E.A. Merritt, W.C. Van Voorhis, D.J. Maly, Development of potent and selective plasmodium falciparum calcium-dependent protein kinase 4 (PfCDPK4) inhibitors that block the transmission of malaria to mosquitoes, *Eur. J. Med. Chem.* 74 (2014) 562–573.
- [3] R.C. Murphy, K.K. Ojo, E.T. Larson, A. Castellanos-Gonzalez, B.G. Perera, K.R. Keyloun, J.E. Kim, J.G. Bhandari, N.R. Muller, C.L. Verlinde, A.C. White Jr., E.A. Merritt, W.C. Van Voorhis, D.J. Maly, Discovery of potent and selective inhibitors of calcium-dependent protein kinase 1 (CDPK1) from *C. parvum* and *T. gondii*, *ACS Med. Chem. Lett.* 1 (2010) 331–335.
- [4] S.M. Johnson, R.C. Murphy, J.A. Geiger, A.E. DeRoche, Z. Zhang, K.K. Ojo, E.T. Larson, B.G. Perera, E.J. Dale, P. He, M.C. Reid, A.M. Fox, N.R. Mueller, E.A. Merritt, E. Fan, M. Parsons, W.C. Van Voorhis, D.J. Maly, Development of toxoplasma gondii calcium-dependent protein kinase 1 (TgCDPK1) inhibitors with potent anti-toxoplasma activity, *J. Med. Chem.* 55 (2012) 2416–2426.
- [5] P. Cohen, Protein kinases—the major drug targets of the twenty-first century? *Nat. Rev. Drug Discov.* 1 (2002) 309–315.
- [6] P. Cohen, D.R. Alessi, Kinase drug discovery—what's next in the field? *ACS Chem. Biol.* 8 (2013) 96–104.
- [7] C.M. Gower, M.E. Chang, D.J. Maly, Bivalent inhibitors of protein kinases, *Crit. Rev. Biochem. Mol. Biol.* 49 (2014) 102–115.
- [8] V. Lamba, I. Ghosh, New directions in targeting protein kinases: focusing upon true allosteric and bivalent inhibitors, *Curr. Pharm. Des.* 18 (2012) 2936–2945.
- [9] T. Genda, M. Sakamoto, T. Ichida, H. Asakura, M. Kojiro, S. Narumiya, S. Hirohashi, Cell motility mediated by rho and Rho-associated protein kinase plays a critical role in intrahepatic metastasis of human hepatocellular carcinoma, *Hepatology* 30 (1999) 1027–1036.
- [10] M. Takamura, M. Sakamoto, T. Genda, T. Ichida, H. Asakura, S. Hirohashi, Inhibition of intrahepatic metastasis of human hepatocellular carcinoma by Rho-associated protein kinase inhibitor Y-27632, *Hepatology* 33 (2001) 577–581.
- [11] T. Ishizaki, M. Maekawa, K. Fujisawa, K. Okawa, A. Iwamatsu, A. Fujita, N. Watanabe, Y. Saito, A. Kakizuka, N. Morii, S. Narumiya, The small GTP-binding protein Rho binds to and activates a 160 kDa Ser/Thr protein kinase homologous to myotonic dystrophy kinase, *EMBO J.* 15 (1996) 1885–1893.
- [12] T. Leung, E. Manser, L. Tan, L. Lim, A novel serine/threonine kinase binding the Ras-related RhoA GTPase which translocates the kinase to peripheral membranes, *J. Biol. Chem.* 270 (1995) 29051–29054.
- [13] T. Matsui, M. Amano, T. Yamamoto, K. Chihara, M. Nakafuku, M. Ito, T. Nakano, K. Okawa, A. Iwamatsu, K. Kaibuchi, Rho-associated kinase, a novel serine/

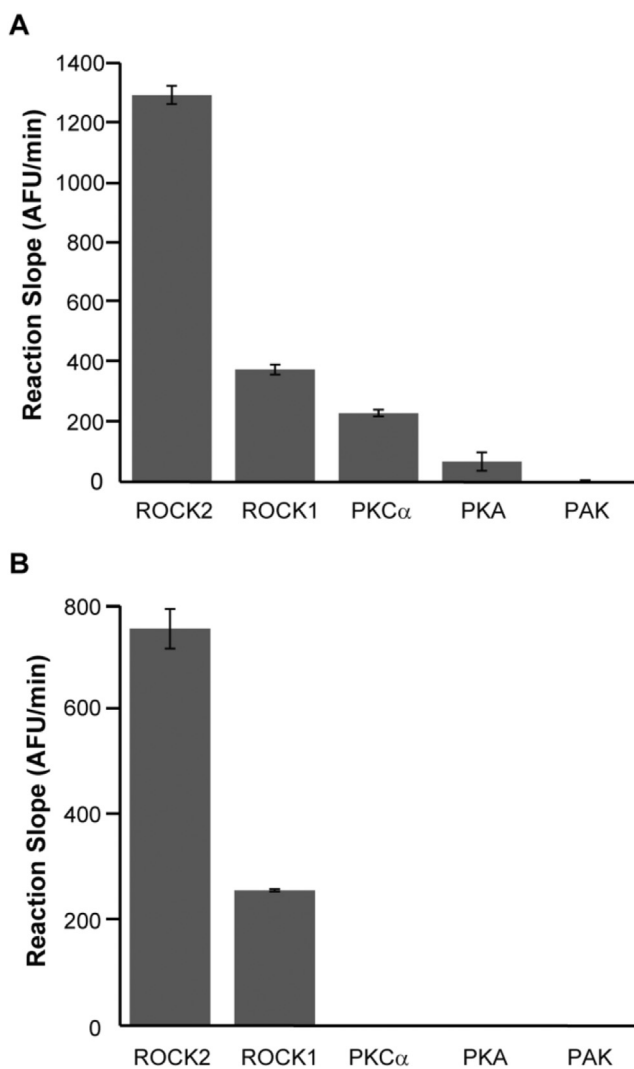


**Fig. 7.** Selectivity of ROCK-S1 among a panel of protein kinases. (A) The phosphorylation of ROCK-S1 (5  $\mu$ M) in the presence of the indicated enzyme (10 nM). (B) The same as panel A except the off-target inhibitors PK1tide (0.4  $\mu$ M), PKC inhibitor peptide (4  $\mu$ M), GF109203X (5  $\mu$ M), and calmidazolium (4  $\mu$ M) are included.

- threonine kinase, as a putative target for small GTP binding protein Rho, *EMBO J.* 15 (1996) 2208–2216.
- [14] G. Manning, D.B. Whyte, R. Martinez, T. Hunter, S. Sudarsanam, The protein kinase complement of the human genome, *Science* 298 (2002) 1912–1934.
- [15] K. Ohashi, K. Nagata, M. Maekawa, T. Ishizaki, S. Narumiya, K. Mizuno, Rho-associated kinase ROCK activates LIM-kinase 1 by phosphorylation at threonine 508 within the activation loop, *J. Biol. Chem.* 275 (2000) 3577–3582.
- [16] T. Sumi, K. Matsumoto, T. Nakamura, Specific activation of LIM kinase 2 via phosphorylation of threonine 505 by ROCK, a Rho-dependent protein kinase, *J. Biol. Chem.* 276 (2001) 670–676.
- [17] K. Kimura, M. Ito, M. Amano, K. Chihara, Y. Fukata, M. Nakafuku, B. Yamamori, J. Feng, T. Nakano, K. Okawa, A. Iwamatsu, K. Kaibuchi, Regulation of myosin sensitization by Rho and Rho-associated kinase (Rho-kinase), *Science* 273 (1996) 245–248.
- [18] G. Totsukawa, Y. Yamakita, S. Yamashiro, D.J. Hartshorne, Y. Sasaki, F. Matsumura, Distinct roles of ROCK (Rho-kinase) and MLCK in spatial regulation of MLC phosphorylation for assembly of stress fibers and focal adhesions in 3T3 fibroblasts, *J. Cell Biol.* 150 (2000) 797–806.
- [19] A.J. Ridley, Rho GTPases and cell migration, *J. Cell Sci.* 114 (2001) 2713–2722.
- [20] M. Uehata, T. Ishizaki, H. Satoh, T. Ono, T. Kawahara, T. Morishita, H. Tamakawa, K. Yamagami, J. Inui, M. Maekawa, S. Narumiya, Calcium sensitization of smooth muscle mediated by a Rho-associated protein kinase in hypertension, *Nature* 389 (1997) 990–994.
- [21] C.J. Hastie, H.J. McLaughlan, P. Cohen, Assay of protein kinases using radiolabeled ATP: a protocol, *Nat. Protoc.* 1 (2006) 968–971.
- [22] Y. Jia, C.M. Quinn, S. Kwak, R.V. Talanian, Current in vitro kinase assay technologies: the quest for a universal format, *Curr. Drug Discov. Technol.* 5 (2008) 59–69.
- [23] J.M. Kolb, G. Yamanaka, S.P. Manly, Use of a novel homogeneous fluorescent technology in high throughput screening, *J. Biomol. Screen* 1 (1996) 203–210.
- [24] N. Ohmi, J.M. Wingfield, H. Yazawa, O. Inagaki, Development of a homogeneous time-resolved fluorescence assay for high throughput screening to identify Lck inhibitors: comparison with scintillation proximity assay and streptavidin-coated plate assay, *J. Biomol. Screen* 5 (2000) 463–470.
- [25] G. Warner, C. Illy, L. Pedro, P. Roby, R. Bosse, Alphascreen kinase HTS platforms, *Curr. Med. Chem.* 11 (2004) 721–730.
- [26] J.A. Gonzalez-Vera, Probing the kinome in real time with fluorescent peptides, *Chem. Soc. Rev.* 41 (2012) 1652–1664.
- [27] D.S. Lawrence, Q.Z. Wang, Seeing is believing: peptide-based fluorescent sensors of protein tyrosine kinase activity, *ChemBioChem* 8 (2007) 373–378.
- [28] D.M. Rothman, M.D. Shults, B. Imperiali, Chemical approaches for investigating phosphorylation in signal transduction networks, *Trends Cell Biol.* 15 (2005) 502–510.
- [29] M.D. Shults, D. Carrico-Moniz, B. Imperiali, Optimal Sox-based fluorescent chemosensor design for serine/threonine protein kinases, *Anal. Biochem.* 352 (2006) 198–207.
- [30] A.K. Devkota, M. Warthaka, R. Edupuganti, C.D.J. Tavares, W.H. Johnson, B. Ozpolat, E.J. Cho, K.N. Dalby, High-throughput screens for eEF-2 kinase, *J. Biomol. Screen* 19 (2014) 445–452.
- [31] S. Balakrishnan, N.J. Zondlo, Design of a protein kinase-inducible domain, *J. Am. Chem. Soc.* 128 (2006) 5590–5591.
- [32] S.C. Zondlo, F. Gao, N.J. Zondlo, Design of an encodable tyrosine kinase-inducible domain: detection of tyrosine kinase activity by terbium luminescence, *J. Am. Chem. Soc.* 132 (2010) 5619–5621.
- [33] K.D. Green, M.K.H. Pflum, Exploring kinase cosubstrate promiscuity: monitoring kinase activity through dansylation, *ChemBioChem* 10 (2009) 234–237.
- [34] M.D. Shults, B. Imperiali, Versatile fluorescence probes of protein kinase activity, *J. Am. Chem. Soc.* 125 (2003) 14248–14249.
- [35] M.D. Shults, K.A. Janes, D.A. Lauffenburger, B. Imperiali, A multiplexed homogeneous fluorescence-based assay for protein kinase activity in cell lysates, *Nat. Methods* 2 (2005) 277–283.
- [36] E. Lukovic, J.A. Gonzalez-Vera, B. Imperiali, Recognition-domain focused chemosensors: versatile and efficient reporters of protein kinase activity, *J. Am. Chem. Soc.* 130 (2008) 12821–12827.
- [37] E. Lukovic, E. Vogel Taylor, B. Imperiali, Monitoring protein kinases in cellular media with highly selective chimeric reporters, *Angew. Chem. Int. Ed.* 48 (2009) 6828–6831.
- [38] L.B. Peterson, M.B. Yaffe, B. Imperiali, Selective mitogen activated protein kinase activity sensors through the application of directionally programmable D domain motifs, *Biochemistry* 53 (2014) 5771–5778.
- [39] C.I. Stains, E. Lukovic, B. Imperiali, A p38alpha-selective chemosensor for use in unfractionated cell lysates, *ACS Chem. Biol.* 6 (2011) 101–105.
- [40] D.A. Szalewski, J.R. Beck, C.I. Stains, Design, synthesis, and evaluation of a selective chemosensor for leucine-rich repeat kinase 2, *Bioorg. Med. Chem. Lett.* 24 (2014) 5648–5651.
- [41] J.R. Beck, L.B. Peterson, B. Imperiali, C.I. Stains, Quantification of protein kinase enzymatic activity in unfractionated cell lysates using CSox-Based Sensors, *Curr. Protoc. Chem. Biol.* 6 (2014) 135–156.
- [42] A. Fersht, *Structure and Mechanism in Protein Science: a Guide to Enzyme Catalysis and Protein Folding*, W.H. Freeman, New York, 1999.
- [43] J.H. Kang, D. Asai, A. Tsuchiya, T. Mori, T. Niidome, Y. Katayama, Peptide substrates for Rho-associated kinase 2 (Rho-kinase 2/ROCK2), *PLoS One* 6 (2011) e22699.
- [44] D. Vigil, T.Y. Kim, A. Plachco, A.J. Garton, L. Castaldo, J.A. Pachter, H. Dong, X. Chen, B. Tokar, S.L. Campbell, C.J. Der, ROCK1 and ROCK2 are required for non-small cell lung cancer anchorage-independent growth and invasion, *Cancer Res.* 72 (2012) 5338–5347.
- [45] J.H. Zhang, T.D.Y. Chung, K.R. Oldenburg, A simple statistical parameter for use in evaluation and validation of high throughput screening assays, *J. Biomol. Screen* 4 (1999) 67–73.
- [46] K.B. Goodman, H.F. Cui, S.E. Dowdell, D.E. Gaitanopoulos, R.L. Ivy, C.A. Sehon, R.A. Stavenger, G.Z. Wang, A.Q. Viet, W.W. Xu, G.S. Ye, S.F. Semus, C. Evans, H.E. Fries, L.J. Jolivet, R.B. Kirkpatrick, E. Dul, S.S. Khandekar, T. Yi, D.K. Jung, L.L. Wright, G.K. Smith, D.J. Behm, R. Bentley, C.P. Doe, E.D. Hu, D. Lee, Development of dihydropyridone indazole amides as selective Rho-kinase inhibitors, *J. Med. Chem.* 50 (2007) 6–9.
- [47] R.J. Nichols, N. Dzamko, J.E. Hutti, L.C. Cantley, M. Deak, J. Moran, P. Bamorough, A.D. Reith, D.R. Alessi, Substrate specificity and inhibitors of LRRK2, a protein kinase mutated in Parkinson's disease, *Biochem. J.* 424 (2009) 47–60.
- [48] T. Asano, I. Ikegaki, S. Satoh, Y. Suzuki, M. Shibuya, M. Takayasu, H. Hidaka, Mechanism of action of a novel antispasmodic drug, HA1077, *J. Pharmacol. Exp. Ther.* 241 (1987) 1033–1040.
- [49] M. Arai, Y. Sasaki, R. Nozawa, Inhibition by the protein kinase inhibitor HA1077 of the activation of NADPH oxidase in human neutrophils, *Biochem. Pharmacol.* 46 (1993) 1487–1490.
- [50] S.P. Davies, H. Reddy, M. Caivano, P. Cohen, Specificity and mechanism of action of some commonly used protein kinase inhibitors, *Biochem. J.* 351 (2000) 95–105.
- [51] J. Bain, L. Plater, M. Elliott, N. Shpiro, C.J. Hastie, H. McLaughlan, I. Klevernic, J.S.C. Arthur, D.R. Alessi, P. Cohen, The selectivity of protein kinase inhibitors: a further update, *Biochem. J.* 408 (2007) 297–315.
- [52] J.G. Christensen, R. Schreck, J. Burrows, P. Kuruganti, E. Chan, P. Le, J. Chen, X.Y. Wang, L. Ruslim, R. Blake, K.E. Lipson, J. Ramphal, S. Do, J.R.J. Cui, J.M. Cherrington, D.B. Mendel, A selective small molecule inhibitor of c-Met kinase inhibits c-Met-dependent phenotypes in vitro and exhibits cytoreductive antitumor activity in vivo, *Cancer Res.* 63 (2003) 7345–7355.
- [53] R. Waelchli, B. Bollbuck, C. Bruns, T. Buhl, J. Eder, R. Felfel, R. Hersperger, P. Janser, L. Revesz, H.G. Zerwes, A. Schlabach, Design and preparation of 2-benzamido-pyrimidines as inhibitors of IKK, *Bioorg. Med. Chem. Lett.* 16 (2006) 108–112.
- [54] C.I. Stains, N.C. Tedford, T.C. Walkup, E. Lukovic, B.N. Goguen, L.G. Griffith, D.A. Lauffenburger, B. Imperiali, Interrogating signaling nodes involved in cellular transformations using kinase activity probes, *Chem. Biol.* 19 (2012) 210–217.
- [55] M. Warthaka, C.H. Adelman, T.S. Kaoud, R. Edupuganti, C.L. Yan, W.H. Johnson, S. Ferguson, C.D. Tavares, L.J. Pence, E.V. Anslyn, P.Y. Ren, K.Y. Tsai, K.N. Dalby, Quantification of a pharmacodynamic ERK end point in Melanoma cell lysates: toward personalized precision medicine, *ACS Med. Chem. Lett.* 6 (2015) 47–52.

## Supplementary Material

### A Real-Time, Fluorescence-Based Assay for Rho-Associated Protein Kinase Activity

Maia I. Kelly<sup>3</sup>, Tyler J. Bechtel<sup>3,1</sup>, D. Rajasekhar Reddy<sup>2</sup>, Erome D. Hankore, Jon R. Beck, and Cliff I. Stains\*

Department of Chemistry, University of Nebraska – Lincoln, Lincoln, Nebraska 68588, United States

#### Table of Contents

Table S1 .....	57
Table S2 .....	58
Table S3 .....	59
Figure S1 .....	62
Figure S2.....	63

**Table S1**

ESI-MS data for ROCK sensors.

Peptide	Calculated Mass [M+xH] <sup>x+</sup>	Observed Mass [M+xH] <sup>x+</sup>
ROCK-S1	[M+2H] <sup>2+</sup> : 1202.9	1202.7
ROCK-P1	[M+2H] <sup>2+</sup> : 1243.0	1243.5
ROCK-S2	[M+2H] <sup>2+</sup> : 1173.6	1173.9
ROCK-P2	[M+2H] <sup>2+</sup> : 1213.5	1213.9

**Table S2**

Fold fluorescence enhancements of ROCK-S1 and ROCK-S2 constructs as a function of Mg<sup>2+</sup> and ATP concentrations.

Peptide	Mg <sup>2+</sup> (mM)	Fold Fluorescence Enhancements <sup>a</sup>	
		0.1 mM ATP	1.0 mM ATP
ROCK-P1	10	2.7	2.1
	20	2.5	2.0
	40	2.0	1.8
ROCK-P2	3.5	4.9	3.5
	7.0	6.1	6.0
	10.5	7.0	6.5

<sup>a</sup>Fold fluorescence enhancements were determined as described in Table 1.

**Table S3**

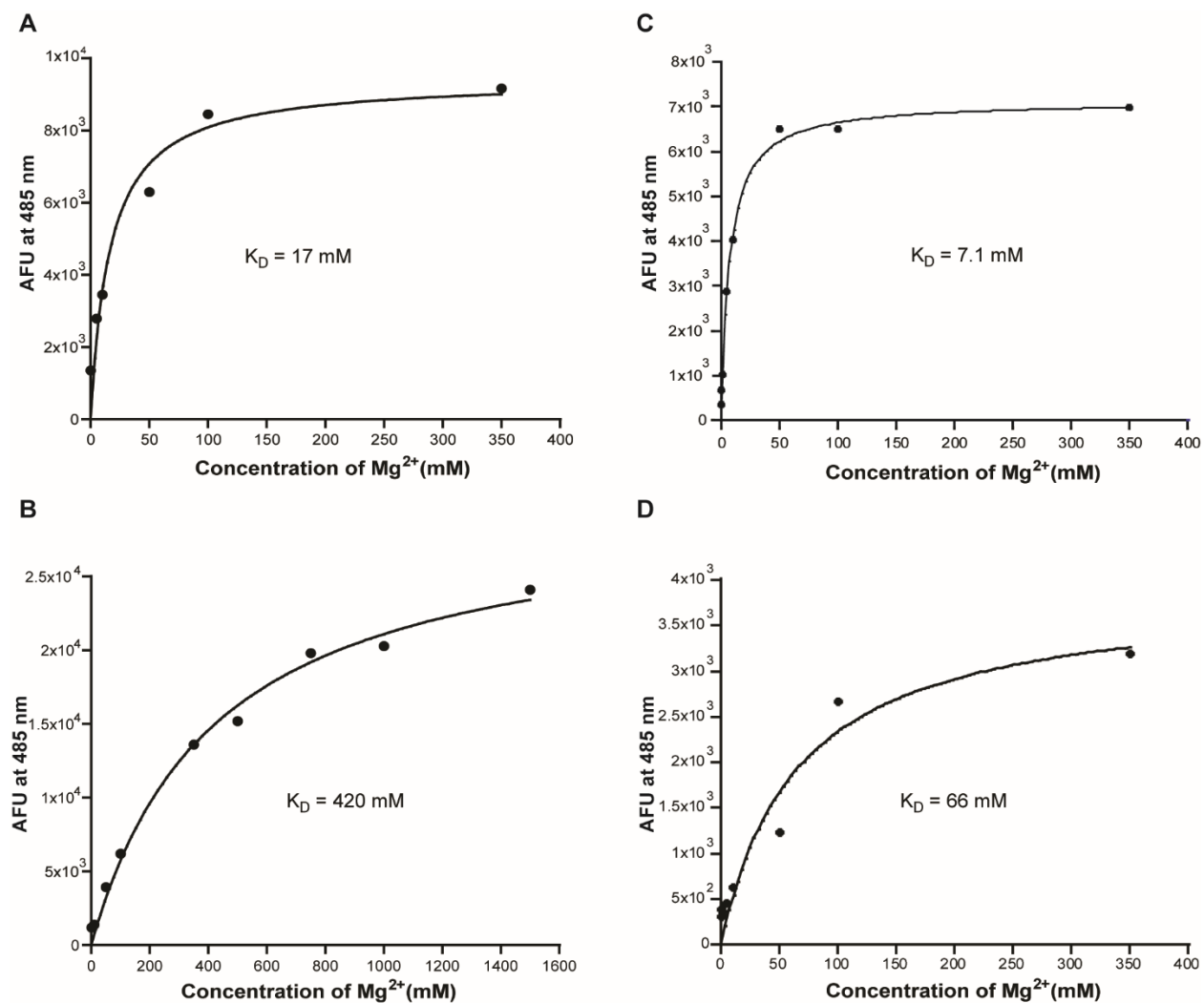
Complete list of inhibitors used for HTS.

<b>Identifier</b>	<b>Inhibitor (10 <math>\mu</math>M)</b>	<b>% Inhibition</b>	<b>Std. Dev. (%)</b>
<b>A1</b>	GSK 429286	100	0.12
<b>A2</b>	ML 9	22	0.82
<b>A3</b>	NH 124	11	0.49
<b>A4</b>	Fasudil	66	0.39
<b>A5</b>	GF109203x	31	1.00
<b>A6</b>	Genistein	4	0.26
<b>A7</b>	LY294002	3	0.63
<b>A8</b>	U0126	3	0.33
<b>A9</b>	PD98059	3	0.30
<b>A10</b>	Y-27632	80	0.22
<b>B1</b>	No Inhibitor Control	-1	1.12
<b>B2</b>	Olomoucine	16	0.83
<b>B3</b>	LFM-A13	14	0.62
<b>B4</b>	ZM 336372	10	0.60
<b>B5</b>	ZM 449829	7	0.20
<b>B6</b>	ZM 39923	9	0.55
<b>B7</b>	GW 5074	52	2.26
<b>B8</b>	PP1	5	0.36
<b>B9</b>	SB 203580	12	0.18
<b>B10</b>	(-)-Tarreic acid	8	0.36
<b>C1</b>	PP 2	22	1.82
<b>C2</b>	SU 4312	21	1.25
<b>C3</b>	SP 600125	3	2.90
<b>C4</b>	Purvalanol A	13	0.49
<b>C5</b>	Purvanol B	16	0.47

<b>C6</b>	KU 55933	8	0.37
<b>C7</b>	AG 490	28	1.42
<b>C8</b>	SB 216763	8	0.58
<b>C9</b>	SB 415286	14	0.46
<b>C10</b>	Arctigenin	7	0.70
<b>D1</b>	NSC 693868	28	2.14
<b>D2</b>	SB 239063	21	1.24
<b>D3</b>	SL 327	21	1.70
<b>D4</b>	Ro 31-8220	55	0.97
<b>D5</b>	Aminopurvalanol A	21	1.29
<b>D6</b>	API-2	11	0.85
<b>D7</b>	GW 441756	17	1.38
<b>D8</b>	GW 583340	22	0.92
<b>D9</b>	Ro 08-2750	44	0.59
<b>D10</b>	TBB	11	0.09
<b>E1</b>	hexabromocyclohexane	21	1.32
<b>E2</b>	HA 1100	68	0.37
<b>E3</b>	BIBX 1382	23	1.06
<b>E4</b>	CGP 53353	15	1.36
<b>E5</b>	Arcyriaflavin A	-9	1.02
<b>E6</b>	ZM 447439	20	0.86
<b>E7</b>	ER 27319	15	0.35
<b>E8</b>	ZM 323881	12	0.89
<b>E9</b>	ZM 306416	11	0.24
<b>E10</b>	IKK 16	81	0.87
<b>F1</b>	Ki 8751	24	1.39
<b>F2</b>	10-DEBC	21	0.79
<b>F3</b>	TPCA-1	22	0.53
<b>F4</b>	SB 218078	-26	6.40

<b>F5</b>	SB 202190	18	1.37
<b>F6</b>	PD 198306	13	0.67
<b>F7</b>	Ryuvidine	31	1.34
<b>F8</b>	IMD 0354	14	0.67
<b>F9</b>	CGK 733	11	0.20
<b>F10</b>	PHA 665752	85	0.85
<b>G1</b>	PD 407824	18	1.60
<b>G2</b>	LY 364974	17	1.08
<b>G3</b>	CGP 57380	16	1.21
<b>G4</b>	PQ 401	14	1.38
<b>G5</b>	PI 828	13	1.15
<b>G6</b>	NU 7026	12	0.90
<b>G7</b>	D4476	-23	5.10
<b>G8</b>	EO 1428	10	1.18
<b>G9</b>	H 89	76	1.28
<b>G10</b>	FPA 124	9	0.88
<b>H1</b>	GWn843682X	14	2.22
<b>H2</b>	Iressa	15	2.03
<b>H3</b>	SU 5416	10	1.73
<b>H4</b>	1-Naphthyl PP1	8	1.81
<b>H5</b>	GSK 650394	19	2.23
<b>H6</b>	BIO	5	1.66
<b>H7</b>	SD 208	11	1.10
<b>H8</b>	Compound 401	6	1.28
<b>H9</b>	BI 78D3	8	1.21
<b>H10</b>	SC 514	8	1.05

Figure S1



Fluorescence of ROCK-P1 (A), ROCK-S1 (B), ROCK-P2 (C), and ROCK-S2 (D) as a function of  $Mg^{2+}$  concentration.

**Figure S2**

A significant proportion (58%) of ROCK2 activity is retained in the presence (+) of the inhibitor cocktail (0.4  $\mu$ M PKItide, 4  $\mu$ M PKC inhibitor peptide, 5  $\mu$ M GF109203X, and 4  $\mu$ M calmidazolium) compared to reactions performed without inhibitors (-).

## References

1. Manning, G., Whyte, D. B., Martinez, R., Hunter, T., and Sudarsanam, S. The protein kinase complement of the human genome. *Science*. **298**, 1912-1934. (2002)
2. Blume-Jensen, P. and T. Hunter. Oncogenic kinase signaling. *Nature*. **411**(6835), 355-365. (2001)
3. Paulsen, C.E., et al. Peroxide-dependent sulfenylation of the EGFR catalytic site enhances kinase activity. *Nat Chem Biol* **8**, 57-64. (2012)
4. Lahiry, P., A. Torkamani, et al. Kinase mutations in human disease: interpreting genotype-phenotype relationships. *Nat Rev Genet*. **11**(1), 60-74. (2010)
5. Cohen, P. Protein kinases- the major drug targets of the twenty-first century? *Nat. Rev Drug Discov* **1**(4), 309-315. (2002)
6. Gonzalez-Vera, J. A. Probing the kinome in real time with fluorescent peptides. *Chem Soc Rev* **41**(5), 1652-1664. (2012)
7. Eglen, R. M., et al. The Use of AlphaScreen Technology in HTS: Current Status. *Curr Chem Genomics*, **1**, 2-10. (2008)
8. Shults, M. D. and Imperiali, B. Versatile fluorescence probes of protein kinase activity. *J Am Chem Soc*. **125**(47). 14248-14249. (2003)
9. Haugland, R.P, Spence, M.T.Z., Johnson, I.D., Basey, A. The handbook: a guide to fluorescent probes and labeling technologies. 10th. Molecular Probes; Eugene, OR: 2005
10. Gribble, F. M., G. Loussouarn, et al. A novel method for measurement of submembrane ATP concentration. *J Biol Chem*. **275**(39). 30046-30049. (2000)
11. Lukovic, E., Gonzalez-Vera, J. A., and Imperiali, B. Recognition-domain focused chemosensors: versatile and efficient reporters of protein kinase activity. *J Am Chem Soc*. **130**, 12821-12827. (2008)
12. Lukovic, E., Vogel Taylor, E., and Imperiali, B. Monitoring protein kinases in cellular media with highly selective chimeric reporters. *Angew Chem Int Ed Engl*. **48**, 6828-6831. (2009)
13. Peterson, L. B., Yaffe, M. B., and Imperiali, B. Selective Mitogen Activated Protein Kinase Activity Sensors through the Application of Directionally Programmable D Domain Motifs. *Biochemistry*. **53**, 5771-5778. (2014)
14. Stains, C. I., Tedford, N. C., Walkup, T. C., Lukovic, E., Goguen, B. N., Griffith, L. G., Lauffenburger, D. A., and Imperiali, B. Interrogating Signaling Nodes Involved in Cellular Transformations Using Kinase Activity Probes. *Chem Biol*. **19**, 210-217. (2012)
15. Warthaka, M., Adelman, et. al. Quantification of a Pharmacodynamic ERK End Point in Melanoma Cell Lysates: Toward Personalized Precision Medicine. *ACS Med Chem Lett*. **6**, 47-52. (2015)
16. Devkota, A. K., et. al. High-Throughput Screens for eEF-2 Kinase. *J Biomol Screen*. **19**, 445-452. (2014)
17. Liver Cancer (Hepatocellular Carcinoma). Retrieved from [http://www.hopkinsmedicine.org/liver\\_tumor\\_center/conditions/cancerous\\_liver\\_tumors/hepatocellular\\_carcinoma.html](http://www.hopkinsmedicine.org/liver_tumor_center/conditions/cancerous_liver_tumors/hepatocellular_carcinoma.html)

18. Nagao, T., Inoue, S., Yoshimi, F., Sodeyama, M., Omori, Y., Mizuta, T., Morioka, Y. Postoperative recurrence of hepatocellular carcinoma. *Annals of Surgery*. **211**(1), 28–33. (1990)
19. Genda, T., et al. Cell motility mediated by rho and Rho-associated protein kinase plays a critical role in intrahepatic metastasis of human hepatocellular carcinoma. *Hepatology*. **30**, 1027-1036. (1999)
20. Poste, G, Fidler IJ. The pathogenesis of cancer metastasis. *Nature*, **283**, 139-146 (1980)
21. Nakashima T. Vascular changes and hemodynamics in hepatocellular carcinoma. In: Okuda K, Peter RL, eds. *Hepatocellular Carcinoma*. New York: Wiley, 1976: 169-203.
22. Pearce, Laura R., David Komander, and Dario R. Alessi. The Nuts and Bolts of AGC Protein Kinases. *Nat Rev Mol Cell Biol*. **11**(1), 9-22. (2010)
23. Jia, Y., Quinn, C. M., Kwak, S., and Talanian, R. V. Current in vitro kinase assay technologies: the quest for a universal format. *Curr Drug Discov Technol*. **5**, 59-69. (2008)
24. Ishizaki, T., et al. The small GTP-binding protein Rho binds to and activates a 160 kDa Ser/Thr protein kinase homologous to myotonic dystrophy kinase. *EMBO J*. **15**, 1885-1893. (1996)
25. PDB ID: 4WOT  
Boland, S., et al. Design, Synthesis, and Biological Evaluation of Novel, Highly Active Soft ROCK Inhibitors. *J Med Chem*. **58**, 4309-4324. (2015)
26. Molecular graphics and analyses were performed with the UCSF Chimera package. Chimera is developed by the Resource for Biocomputing, Visualization, and Informatics at the University of California, San Francisco (supported by NIGMS P41-GM103311).
27. Kimura, K., et al. Regulation of myosin phosphatase by Rho and Rho-associated kinase (Rho-kinase). *Science*. **273**, 245-248. (1996)
28. Ohashi, K., et al. Rho-associated kinase ROCK activates LIM-kinase 1 by phosphorylation at threonine 508 within the activation loop. *J Biol Chem*. **275**, 3577-3582. (2000)
29. Kang, J.H., et al. Peptide substrates for Rho-associated kinase 2 (Rho-kinase 2/ROCK2), *PloS One*. **6**, e22699. (2011)
30. Szalewski, D. A., Beck, J. R., and Stains, C. I. Design, synthesis, and evaluation of a selective chemosensor for leucine-rich repeat kinase 2. *Bioorg Med Chem Lett*. **24**, 5648-5651. (2014)
31. Beck, J.R., Peterson, L.B., Imperiali, B., Stains, C.I. Quantification of protein kinase enzymatic activity in unfractionated cell lysates using CSox-Based Sensors. *Curr Protoc Chem Biol*. **6**, 135–156. (2014)
32. Vigil, D., et al. ROCK1 and ROCK2 are required for non-small cell lung cancer anchorage-independent growth and invasion. *Cancer Res*. **72**, 5338–5347 (2012)
33. J.H. Zhang, T.D.Y. Chung, K.R. Oldenburg, A simple statistical parameter for use in evaluation and validation of high throughput screening assays. *J Biomol Screen*. **4**, 67-73. (1999)
34. Goodman, K.B., et al. Development of dihydropyridone indazole amides as selective Rho-kinase inhibitors. *J Med Chem*. **50**, 6-9. (2007)

35. Nichols, R.J., et al. Substrate specificity and inhibitors of LRRK2, a protein kinase mutated in Parkinson's disease. *Biochem J.* **424** 47-60. (2009)
36. Asano, T., et al. Mechanism of action of a novel antivasospasm drug, HA1077. *J. Pharmacol Exp Ther.* **241**(1087), 1033-1040. (1987)
37. Uehata, M. et al. Calcium sensitization of smooth muscle mediated by a Rho-associated protein kinase in hypertension. *Nature.* **389**, 990-994. (1997)
38. Arai, M., Sasaki, Y. Nozawa, R. Inhibition by protein kinase inhibitor HA1077 of the activation of NADPH oxidase in human neutrophils. *Biochem Pharmacol.* **47**, 1487-1490. (1993)
39. J. Bain, L. Plater, M. Elliott, N. Shpiro, C.J. Hastie, H. Mclauchlan, I. Klevernic, J.S.C. Arthur, D.R. Alessi, P. Cohen, The selectivity of protein kinase inhibitors: a further update, *Biochem J.* **408**, 297-315. (2007)
40. S.P. Davies, H. Reddy, M. Caivano, P. Cohen, Specificity and mechanism of action of some commonly used protein kinase inhibitors. *Biochem J.* **351**, 95-105. (2000)
41. S.P. Davies, H. Reddy, M. Caivano, P. Cohen, Specificity and mechanism of action of some commonly used protein kinase inhibitors. *Biochem J.* **351**, 95-105. (2000)
42. Waelchli, R., et al. Design and preparation of 2-benzamido-pyrimidines as inhibitors of IKK, *Bioorg Med Chem Lett.* **16**, 108-112. (2006)
43. Shults, M.D., Janes, K.A., Lauffenburger, D.A., Imperiali, B. A multiplexed homogeneous fluorescence-based assay for protein kinase activity in cell lysates. *Nat Methods.* **2**, 277-283. (2005)
44. Stains, C.I., Lukovic, E., Imperiali, B. A p38alpha-selective chemosensor for use in unfractionated cell lysates. *ACS Chem Biol.* **6**, 101-105. (2011)
45. Ohashi, K., et al. Rho-associated kinase ROCK activates LIM-kinase 1 by phosphorylation at threonine 508 within the activation loop. *J Biol Chem,* **275**, 3577-3582. (2000)
46. Kang, J.H., et al. Peptide substrates for Rho-associated kinase 2 (Rho-kinase 2/ROCK2). *PLoS One.* **6**, e22699. (2011)
47. A. Fersht, Structure and Mechanism in Protein Science: a Guide to Enzyme Catalysis and Protein Folding, W.H. Freeman, New York, 1999.